npj | Biofilms and Microbiomes

www.nature.com/npjbiofilms

ARTICLE OPEN

Daily full spectrum light exposure prevents food allergy-like allergic diarrhea by modulating vitamin D_3 and microbiota composition

Po-Jung Chen[1,2], Toshiaki Nakano[1,2]✉, Chia-Yun Lai[2], Kuei-Chen Chang[1,2], Chao-Long Chen[2] and Shigeru Goto[2,3,4]

The importance of sun exposure on human health is well recognized, and a recent trend in the avoidance of sun exposure has led to the risk of missing the beneficial effects such as vitamin D_3 biogenesis. Vitamin D_3 insufficiency is one of the risk factors for the development of food allergies (FAs), and vitamin D_3 status controls gut homeostasis by modulating the microbiota. This study aimed to explore the impact of daily full spectrum light exposure (phototherapy) on the pathogenesis of FAs. Phototherapy ameliorated allergic diarrhea and improved FA-associated vitamin D_3 insufficiency and dysbiosis. Fecal microbiota transplantation (FMT) of FA donor feces induced allergic diarrhea with OVA-specific IgE elevation in naïve mice. In contrast, FMT of naïve donor feces ameliorated allergic diarrhea in established FA mice, suggesting the involvement of the microbiota composition in FA. Phototherapy is an alternative approach for the prevention of FA-like allergic diarrhea through the modulation of vitamin D_3 status and microbiota composition.

npj Biofilms and Microbiomes (2021)7:41 ; https://doi.org/10.1038/s41522-021-00213-8

INTRODUCTION

Food allergies (FAs) are common in children and adults, and the prevalence of FAs has increased dramatically in the past few decades in westernized countries[1]. FA is considered mainly an IgE-mediated type I (immediate) hypersensitivity, and the continuous sensitization of food allergens may cause mild-to-severe allergic reactions such as dermatitis, gastrointestinal and respiratory distress, and life-threatening anaphylaxis. The traditional treatment approach to FA is the avoidance of allergenic foods, and patients must carry a self-injectable form of epinephrine for emergency treatment of anaphylaxis[2]. In addition to the lack of a complete cure for FAs, the mechanisms of FAs are still uncertain.

There are several theories explaining the increase in FAs, including (1) changes in our food system (e.g., the introduction of genetically modified organisms, the addition of numerous chemicals to our food), (2) the hygiene hypothesis, (3) epigenetics, and (4) delayed allergen exposure[3–7]. In addition, epidemiological evidence has shown that low vitamin D_3 levels in infancy appear to be a risk factor for the development of FAs[8]. Interestingly, pediatric FAs are more prevalent in regions farther away from the equator[9,10]. The negative correlation between the amount of sun exposure immediately after birth and food sensitization[11] as well as the higher frequency of autumn–winter births in FA patients[12] strongly suggest the significance of sun exposure and vitamin D_3 generation in the prevention of FA. However, due to the destruction of the ozone layer in the past few decades[13], we are exposed to large amounts of UVA and UVB, which cause skin aging, damage, and cancer progression[14]. Therefore, there have been many public health recommendations to avoid UV radiation exposure, which may cause significant harm to public health due to vitamin D_3 insufficiency[15].

Since Niels Ryberg Finsen (1860–1904) introduced full spectrum light therapy (short phototherapy) for the treatment of skin disease[16], phototherapy has been applied for many diseases, such as mental disorders[17,18], sleep disorders[19,20], neurological disorders[21,22], and neonatal jaundice[23]. In our previous study, we demonstrated reduced expression of vitamin D_3 in nonalcoholic steatohepatitis (NASH), and daily exposure to full spectrum light and vitamin D_3 supplementation ameliorated NASH progression in rats[24]. This study is the first confirmation of the therapeutic potency of phototherapy and vitamin D_3 supplementation in an animal model of NASH, which clearly builds the basis for subsequent human therapeutic trials for NASH (ClinicalTrials.gov identifier: NCT01571063)[25]. In addition to the clinical impact of phototherapy in terms of the elevation of vitamin D_3 in NASH patients[26], we have demonstrated the therapeutic potential of phototherapy in experimental models of colitis[27] and peritonitis[28]. However, there are no studies applying phototherapy for the prevention of FA.

In addition to the association between vitamin D_3 status and FAs, accumulating evidence suggests the impact of compositional and functional changes in gut microbiota on the dramatic increase in FA prevalence[29–31]. The gut microbiota is recognized as a target for preventive and therapeutic intervention against FAs[32], while limited information is available addressing the therapeutic potential of fecal microbiota transplantation (FMT) for allergic disorders[33]. Vitamin D_3 status controls gut homeostasis by modulating the gut microbiota[34], and a recent study pointed to the modulation of gut microbiota by narrow band UVB light exposure[35]. However, there are no studies exploring the synergistic impact of full spectrum light on vitamin D_3 status and microbiota composition. In this study, we explored the impact of phototherapy on the pathogenesis of OVA-induced FA in mice and discussed the significance of vitamin D_3 status and the fecal microbiota composition in FA.

[1]Graduate Institute of Clinical Medical Sciences, Chang Gung University College of Medicine, Kaohsiung, Taiwan. [2]Liver Transplantation Center, Kaohsiung Chang Gung Memorial Hospital, Kaohsiung, Taiwan. [3]Nobeoka Medical Check Center, Fukuoka Institution of Occupational Health, Nobeoka, Japan. [4]Faculty of Nursing, Josai International University, Togane, Japan. ✉email: nakano33@mail.cgu.edu.tw

RESULTS

Impact of phototherapy on the pathogenesis of FA

An OVA-induced FA model was established to explore whether phototherapy could prevent FA symptoms. As shown in Fig. 1a, allergic diarrhea was confirmed at the 3rd OVA challenge in OVA-sensitized FA mice. The incidence of allergic diarrhea gradually increased after the 3rd OVA challenge and all mice (14/14) showed allergic diarrhea at the 15th OVA challenge in the FA group. Histological data revealed mucosal and submucosal inflammation and shortening of intestinal villi in FA (Fig. 1b). On the other hand, phototherapy reduced the incidence of allergic diarrhea, and the maximum incidence of allergic diarrhea was 33.3% (4/12) at the 9th OVA challenge. The reduced incidence of allergic diarrhea at the 15th OVA challenge (2/12, 16.6%) with phototherapy suggested the potential effect of phototherapy on both the prevention and therapeutics of FA. Histological data clearly revealed the amelioration of allergic inflammation by phototherapy (Fig. 1b).

To further explore the impact of phototherapy on the pathogenesis of FA, we next evaluated FA-associated mucosal mast cell activation in the intestine after the 15th OVA challenge. As shown in Fig. 1c (left), we confirmed the FA-induced accumulation of mucosal mast cells in the intestinal submucosa and lamina propria, while phototherapy suppressed this accumulation. The elevation of mucosal mast cell protease 1 (Mcpt-1) at the mRNA (Supplementary Fig. 1a) and protein (Fig. 1c, right) levels was also observed, thus suggesting the activation and degranulation of intestinal mucosal mast cells during the development of FA. Furthermore, we confirmed systemic elevation of Mcpt-1 in FA, while phototherapy suppressed it (Supplementary Fig. 1b).

Impact of phototherapy on immunoglobulin production in FA

We next evaluated the impact of phototherapy on the expression profiles of total and OVA-specific immunoglobulins after the 15th OVA challenge. As shown in Fig. 2, OVA sensitization and the subsequent OVA challenge significantly induced the elevation of total and OVA-specific IgE and IgG1 levels, suggesting the activation of IgE- and Th2-mediated allergy responses in the FA group. Phototherapy suppressed the elevation of total and OVA-specific IgE and IgG1 levels but slightly induced total and OVA-specific IgG2a expression after OVA challenge, resulting in the amelioration of FA-like allergic diarrhea by daily phototherapy during OVA sensitization and the subsequent OVA challenge.

Impact of phototherapy on T-cell phenotypes and FA-associated pro-Th2 cytokine expression in the intestine

We next explored the impact of phototherapy on T-cell phenotypes in the intestine. As shown in Supplementary Fig. 2, the expression levels of T-bet (Th1), GATA3 (Th2), RoRγt (Th17), and FoxP3 (regulatory T cells) were significantly elevated in the FA intestine, while phototherapy reduced their expression. Phototherapy may ameliorate the activation of both effector T cells and regulatory T cells during OVA-induced allergic diarrhea. We further explored the impact of phototherapy on the intestinal level of the pro-Th2 cytokines IL-25, IL-33, and thymic stromal lymphopoietin (TSLP), which are primarily produced by epithelial cells upon allergen challenge and associated with FA[36]. As shown in Fig. 3, intestinal levels of IL-25, IL-33, and TSLP were significantly increased in the FA group, while phototherapy suppressed their expression in the intestine.

Impact of phototherapy on vitamin D_3 metabolism in FA

To explore the impact of phototherapy on vitamin D_3 status in FA, the serum level of the active form vitamin D_3 (DHVD3) was quantified. As shown in Fig. 4a, vitamin D_3 insufficiency was observed in the FA group. Corresponding to the reduction in serum vitamin D_3, vitamin D receptor (VDR) expression in the intestine was also reduced in the FA group (Fig. 4b). On the other hand, phototherapy could induce the elevation of serum vitamin D_3 in naïve mice (Supplementary Fig. 3a). Therefore, FA mice with phototherapy were able to ameliorate vitamin D_3 insufficiency with higher expression of intestinal VDR than FA mice (Fig. 4). These data were negatively correlated with the expression profiles of total and OVA-specific IgE in FA with/without phototherapy (Fig. 2a).

We next explored the intestinal levels of the vitamin D-metabolizing enzymes sterol 27-hydroxylase (CYP27A1) and 25-hydroxyvitamin D_3-1α hydroxylase (CYP27B1). As shown in Fig. 4c and d, the expression levels of CYP27A1 and CYP27B1 in the intestine were significantly reduced in the FA group compared with the control group. As shown in Supplementary Fig. 3b, phototherapy could induce the expression of intestinal CYP27A1 and CYP27B1 in naïve mice. Therefore, phototherapy could maintain these levels to some extent. These results suggest the involvement of intestinal vitamin D biosynthesis and a VDR-mediated mechanism of action of endogenous vitamin D_3 in the amelioration of FA-like allergic diarrhea by phototherapy. The reduction in intestinal CYP27A1 and CYP27B1 levels may not be due to the sloughing of the epithelial lining from multiple episodes of allergic diarrhea in the FA group because of the similar expression profile of epithelial cell adhesion molecule, a marker for intestinal epithelial cells, in the control, FA, and phototherapy groups (Supplementary Fig. 3c). Taken together, the reduction in CYP27A1 and CYP27B1 is likely associated with FA-like allergic diarrhea.

Impact of phototherapy on oxidative stress and antioxidant defense responses in FA

A recent study mentioned the association between FA and the oxidative stress response[37]. To further explore the impact of phototherapy on oxidative stress and antioxidant defense responses in FA, the intestinal levels of nuclear factor erythroid 2-related factor 2 (Nrf2), a master regulator of the antioxidant machinery, and antioxidant genes such as heme oxygenase-1 (HO-1), superoxide dismutase 1 (SOD1), and SOD2 were evaluated. As shown in Fig. 5a, intestinal Nrf2 expression was elevated in both the FA and phototherapy groups, while FA failed to induce SOD1 and SOD2 (Fig. 5c, d). Intriguingly, phototherapy activated intestinal Nrf2 expression in both naïve and FA mice (Supplementary Fig. 4) followed by the induction of antioxidant genes. Taken together, one of the potential mechanisms for the amelioration of FA by phototherapy may be the modulation of the oxidative stress response by Nrf2 activation.

Impact of phototherapy on the fecal microbiota composition in FA

We performed bacterial taxonomic analysis to investigate the impact of phototherapy on the fecal microbiota composition in FA. As shown in Supplementary Fig. 5a, FA induced a reduction in the phylum *Bacteroidetes* and an elevation in the phylum *Firmicutes*, which correspond to the ratio observed in clinical FA patients[38]. Quantitative real-time PCR analysis also demonstrated an elevation in the *Firmicutes*/*Bacteroidetes* ratio (196.9 ± 129.3, $P < 0.0001$ vs. control: 1.11 ± 0.547) in FA mice (Fig. 6a). In addition, phototherapy maintained a comparable *Firmicutes*/*Bacteroidetes* ratio (1.94 ± 1.71, $P = 0.143$) to the control, suggesting the impact of phototherapy on the maintenance of healthy microbiota. Linear discriminant analysis (LDA) effect size (LEfSe) analysis was then performed to discover biomarkers with significant differences among the three groups. As shown in Supplementary Fig. 5b, the genus *Lachnospiraceae_NK4A136_group* (phylum *Firmicutes*) and family *Peptococcaceae* (phylum *Firmicutes*) were enriched in FA

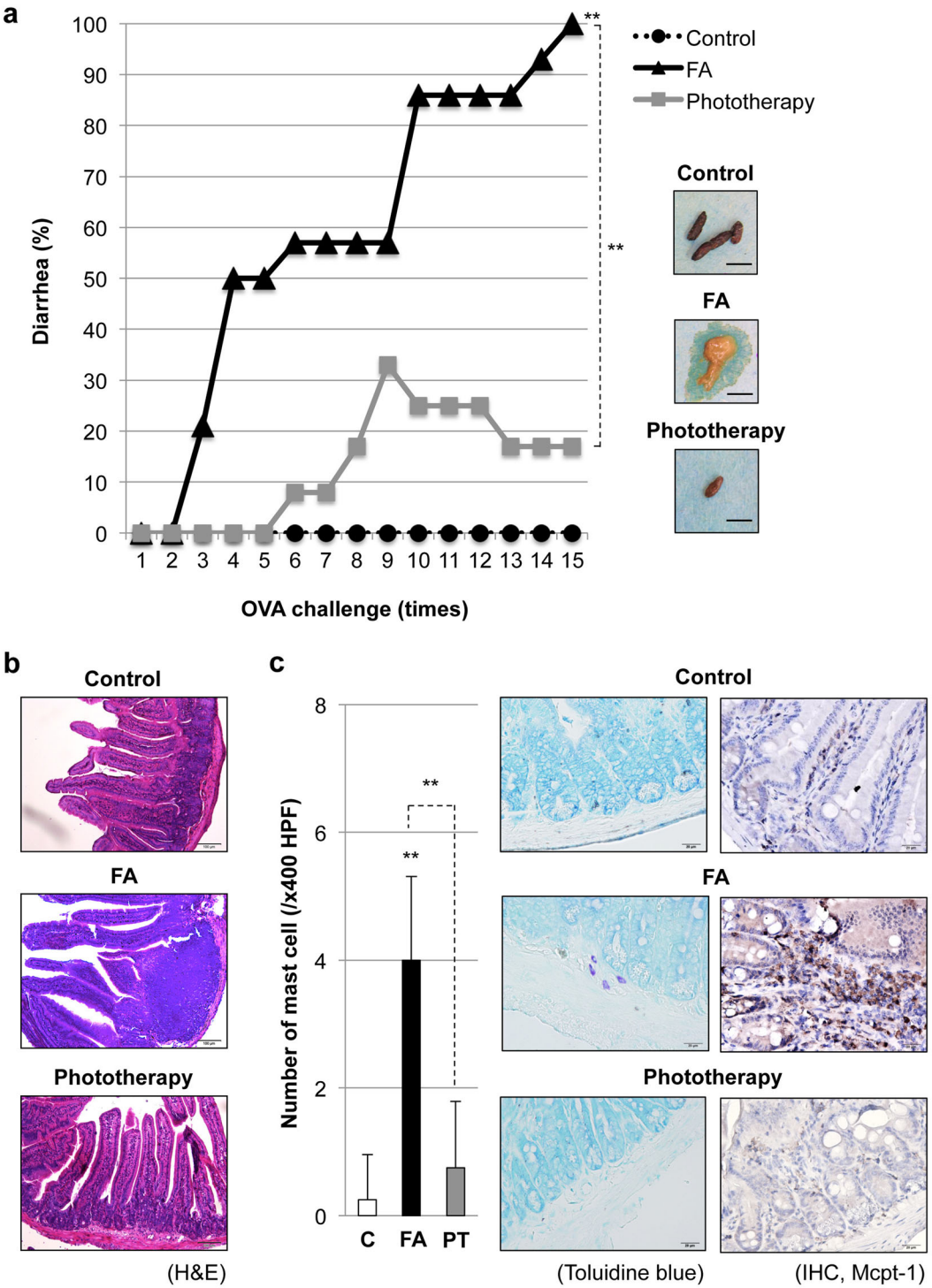

Fig. 1 Impact of phototherapy on the pathogenesis of food allergy (FA). a Establishment of FA mice. Repeated intragastric (i.g.) OVA challenge was performed 15 times in OVA-sensitized BALB/c mice with ($n = 12$) or without phototherapy ($n = 14$). Naïve mice ($n = 8$) without OVA immunization were treated with PBS as a control. Allergic diarrhea was assessed visually by monitoring mice for 30 min after each i.g. exposure. $^{**}P < 0.01$ vs. the control group or the indicated pair (Tukey's multiple comparisons test). Enclosed pictures are representative feces after i.g. OVA challenge in the control, FA, and phototherapy groups. Scale bar: 5 mm. **b** Histological evaluation of the intestines in FA mice. The pictures at ×100 magnification are representative of at least six individuals in each group. H&E hematoxylin and eosin staining. Scale bar: 100 μm. **c** Mucosal mast cell activation in FA mice. Left: mast cells were visualized by toluidine blue staining and counted under a microscope at ×400 magnification. Values are presented as the mean ± SD of at least six individuals in each group. C control, FA food allergy, PT phototherapy. $^{**}P < 0.01$ vs. the control or phototherapy group (Student's *t* test). Right: immunohistochemistry (IHC) for mast cell protease 1 (Mcpt-1). The pictures at ×400 magnification are representative of at least six individuals in each group. Scale bar: 20 μm.

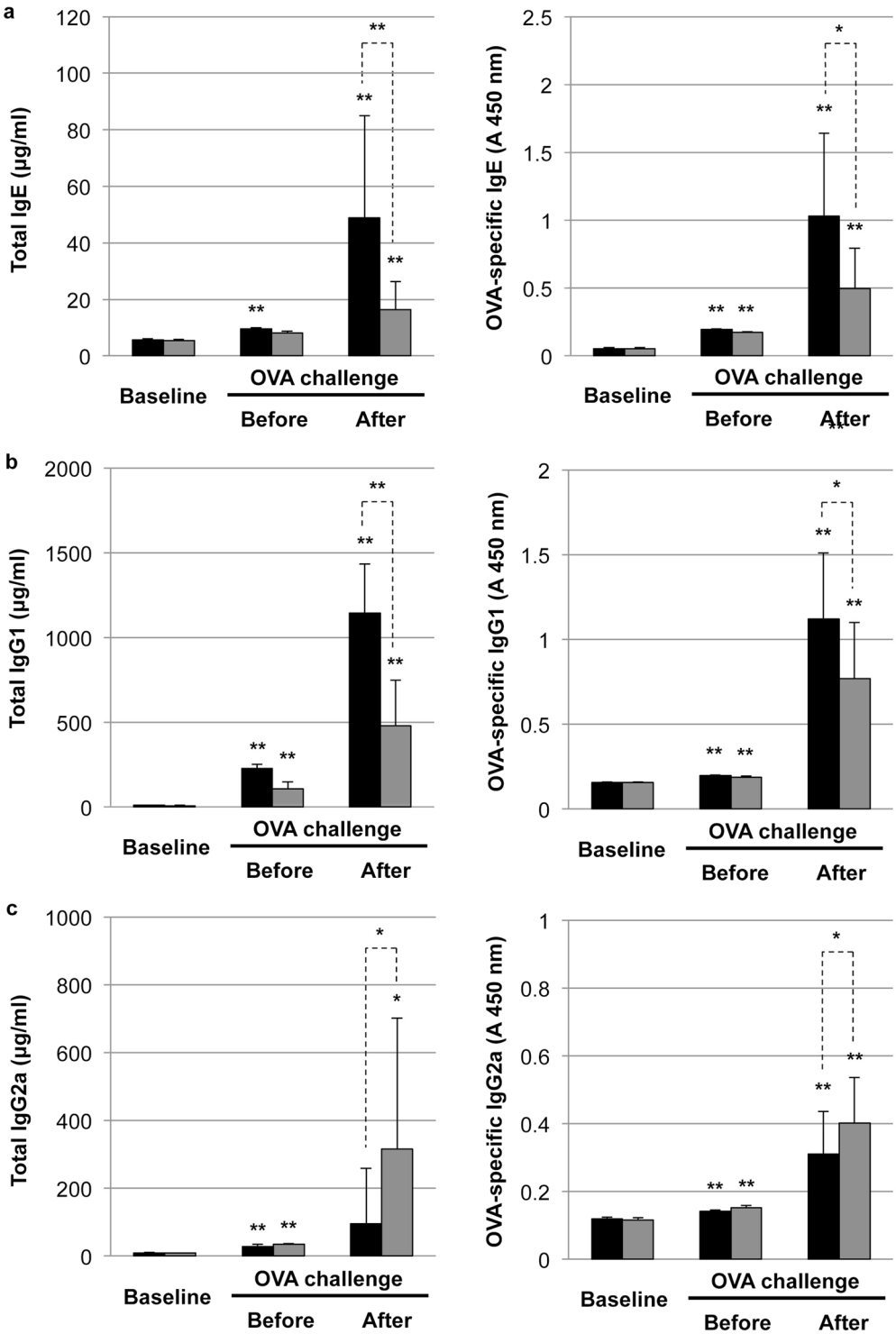

Fig. 2 Impact of phototherapy on immunoglobulin production in food allergy (FA). Serum levels of total or OVA-specific IgE (**a**), IgG1 (**b**), and IgG2a (**c**) in the FA (black bar) and phototherapy (gray bar) group were measured by ELISA. Values are presented as the mean ± SD of at least eight individuals in each group. *, **, $P < 0.05$ and 0.01 vs. baseline or the phototherapy group, respectively (Student's *t* test).

mice. We next performed beta diversity comparison of the gut microbiomes between the FA and phototherapy groups at the genus and species levels. As shown in Fig. 6b, FA significantly increased the genus *Lachnospiraceae_NK4A136_group* ($P = 0.016$). On the other hand, the species *Parabacteroides_goldsteinii* (Phylum *Bacteroidetes*) was enriched in phototherapy-treated mice ($P = 0.014$).

Application of FMT for functional evaluation of FA-associated dysbiosis

We performed FMT to explore whether FA-associated dysbiosis directly transfers FA symptoms in naïve BALB/c mice. As shown in Supplementary Fig. 6a, antibiotics completely removed the original gut microbiota, and FMT with FA donor feces (FA-FMT) successfully introduced FA-associated dysbiosis in naïve BALB/c

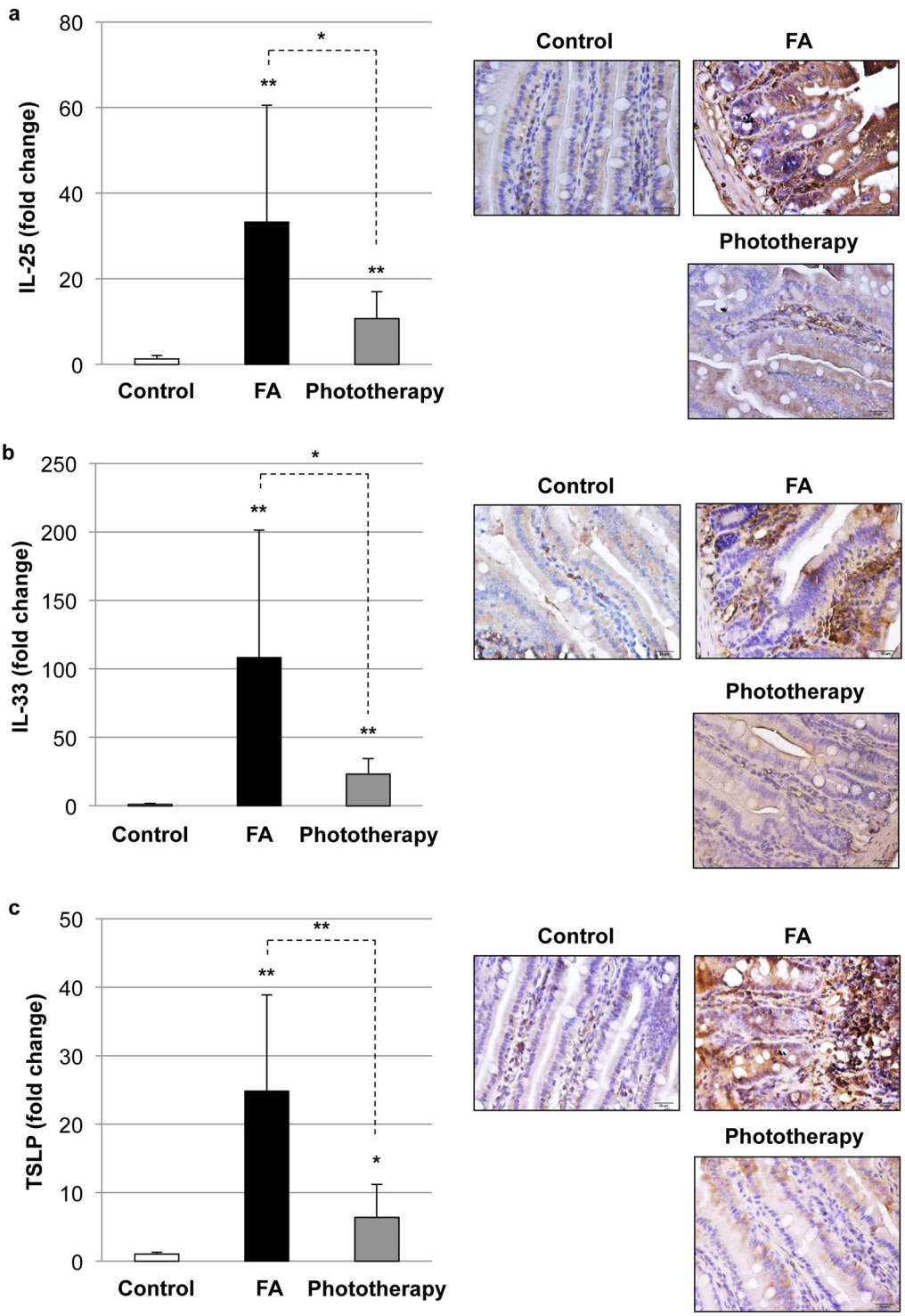

Fig. 3 Impact of phototherapy on food allergy (FA)-associated pro-Th2 cytokine expression. Intestinal levels of IL-25 (**a**), IL-33 (**b**), and thymic stromal lymphopoietin (TSLP) (**c**) were evaluated by quantitative real-time PCR and immunohistochemistry (IHC). Left: values are presented as the mean ± SD of at least eight individuals in each group. *, **, $P < 0.05$ and 0.01 vs. the control or phototherapy group, respectively (Student's *t* test). The pictures at ×400 magnification are representative of at least six individuals in each group. Scale bar: 20 μm.

mice. On the other hand, FMT itself did not affect the expression profiles of circulating vitamin D_3 (Supplementary Fig. 6b) and pro-Th2 cytokines (Supplementary Fig. 6c). As shown in Fig. 7a, allergic diarrhea occurred immediately after the 1st OVA challenge, and 90% (9/10) of FA-FMT mice experienced allergic diarrhea at the 6th OVA challenge. In addition, the incidence of allergic diarrhea in the phototherapy-FMT or control-FMT groups was 50% (5/10) and 30% (3/10), respectively, at the 6th OVA challenge. We confirmed the statistic significance between FA-FMT and control-FMT ($P = 0.0164$). Histological data revealed allergic inflammation and abnormal villous shortening by FA-FMT (Fig. 7b). Although FMT itself did not affect the levels of total and OVA-specific IgE, FA-FMT mice had higher levels of total and OVA-specific IgE after the 6th OVA challenge (Fig. 7c). This evidence suggests the

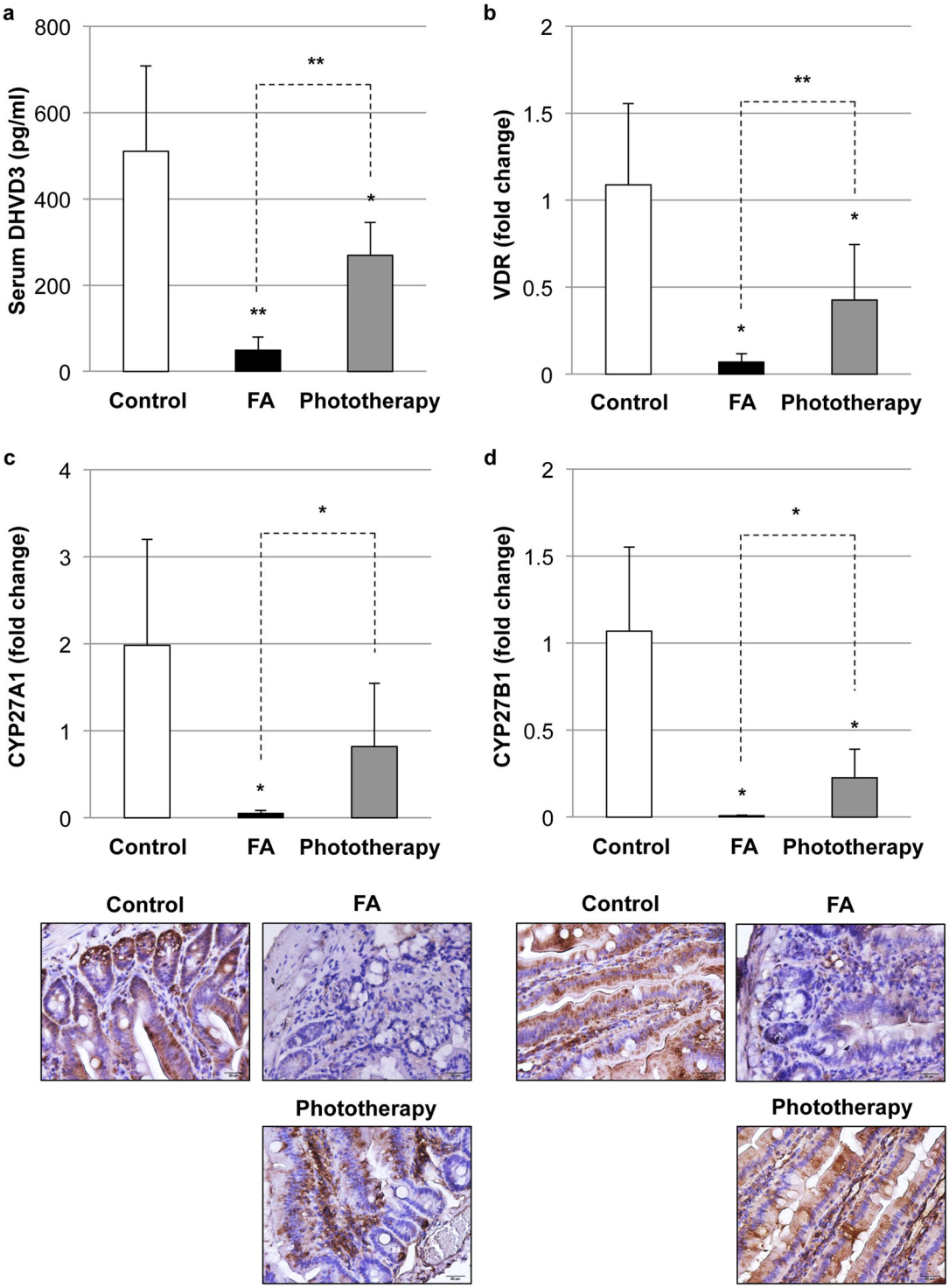

Fig. 4 Impact of phototherapy on vitamin D_3 metabolism in food allergy (FA). a Serum levels of vitamin D_3 were measured by ELISA. Values are presented as the mean ± SD of at least eight individuals in each group. *, **, $P < 0.05$ and 0.01 vs. the control or phototherapy group, respectively (Student's *t* test). Intestinal levels of vitamin D receptor (VDR) (**b**), sterol 27-hydroxylase (CYP27A1) (**c**), and 25-hydroxyvitamin D_3-1α hydroxylase (CYP27B1) (**d**) were evaluated by quantitative real-time PCR and immunohistochemistry (IHC). Values are presented as the mean ± SD of at least six individuals in each group. *, **, $P < 0.05$ and 0.01 vs. the control or phototherapy group, respectively (Student's *t* test). The pictures at ×400 magnification are representative of at least six individuals in each group. Scale bar: 20 μm.

existence of unique microbacteria in FA donor feces for the induction of the OVA-specific IgE response and IgE-mediated allergic diarrhea. We also confirmed vitamin D_3 insufficiency in all FMT groups (Supplementary Fig. 6b) due to the induction of dysbiosis by OVA challenge (data not shown). However, the expression levels of vitamin D_3, CYP27A1, and CYP27B1 in control-FMT and phototherapy-FMT were relatively higher than those in FA-FMT (Supplementary Fig. 6b). Although OVA challenge induced the elevation of intestinal IL-25, IL-33, and TSLP in all FMT groups, the control-FMT and phototherapy-FMT groups had relatively

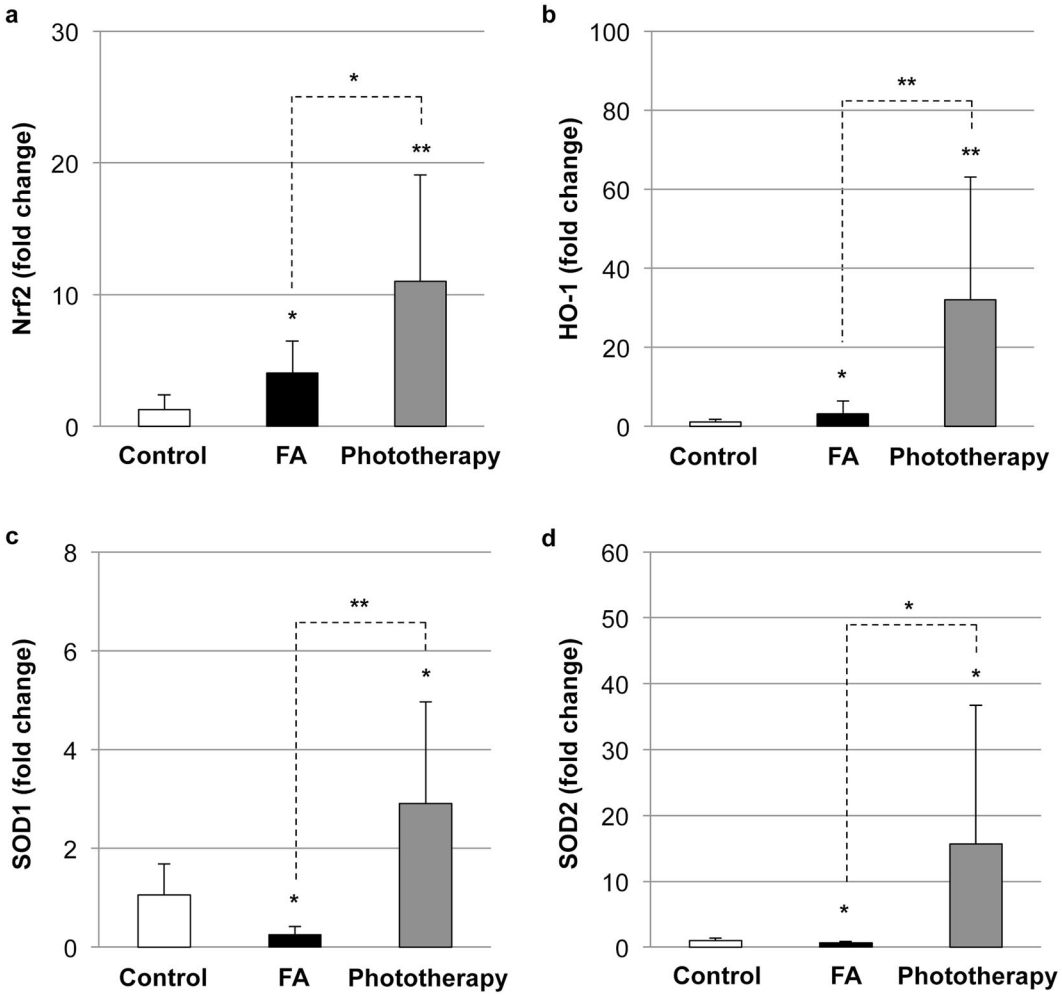

Fig. 5 Impact of phototherapy on oxidative stress and antioxidant defense in food allergy (FA). Intestinal levels of nuclear factor erythroid 2-related factor 2 (Nrf2) (**a**), heme oxygenase-1 (HO-1) (**b**), superoxide dismutase 1 (SOD1) (**c**), and SOD2 (**d**) were evaluated by quantitative real-time PCR. Values are presented as the mean ± SD of at least eight individuals in each group. *, **, $P < 0.05$ and 0.01 vs. the control or phototherapy group, respectively (Student's *t* test).

lower expression of IL-33 and TSLP than FA-FMT (Supplementary Fig. 6c). We also confirmed the relatively higher expression of Nrf2 by phototherapy-FMT treatment (Supplementary Fig. 7a), resulting in a lower incidence of allergic diarrhea.

Application of FMT for therapeutic modulation of diseased microbiota

To examine the impact of gut microbiota on FA from another perspective, we performed control-FMT to FA mice. As expected, control-FMT improved FA-associated dysbiosis by modulating the *Firmicutes*/*Bacteroidetes* ratio (0.726 ± 0.405) (Supplementary Fig. 8a). Similar to the previous observation (Supplementary Fig. 6b), FMT itself did not recover vitamin D_3 insufficiency (Supplementary Fig. 8b) and maintained intestinal pro-Th2 cytokine expression in FA mice (Supplementary Fig. 8c). As shown in Fig. 8a, control-FMT mice showed delayed onset of allergic diarrhea. Although allergic diarrhea was observed at the 6th OVA challenge in control-FMT mice, histological data revealed a better intestinal morphology in FA mice receiving control-FMT (Fig. 8b). We also confirmed the reduced expression of total and OVA-specific IgE by control-FMT (Fig. 8c). The replacement of diseased microbiota with healthy microbiota by control-FMT reduced the elevation of intestinal IL-25, IL-33, and TSLP but enhanced Nrf2 expression (Supplementary Fig. 7b). This evidence suggests the therapeutic potential of FMT for FA-like allergic diarrhea partly through the modulation of gut microbiota.

DISCUSSION

The importance of sunlight exposure on mental and physical conditions has been well recognized since time immemorial. However, promoting the avoidance of sunlight exposure in recent years has led to the risk of not receiving beneficial effects such as vitamin D_3 biogenesis. In this study, we used full spectrum light, which may reduce the risk of excessive UV exposure, as a light source for phototherapy and demonstrated its beneficial impact on FA-like allergic diarrhea (Figs. 1–3).

Although the mode of action of phototherapy was not fully clarified in this study, one of the potential mechanisms underlining the beneficial impact of phototherapy should be the improvement in FA-associated vitamin D_3 insufficiency. FA mice showed a reduction in intestinal VDR, CYP27A1, and CYP27B1 expression, resulting in the impairment of vitamin D biosynthesis and VDR-mediated mechanism of action of endogenous vitamin D_3. On the other hand, phototherapy could prevent the FA-associated reduction in systemic vitamin D_3 and intestinal genes for vitamin D_3 metabolism (Fig. 4). OVA-sensitized *Cyp27b1*-knockout mice had an increase in total and OVA-specific IgE concentrations[39], suggesting the regulation of the IgE-mediated

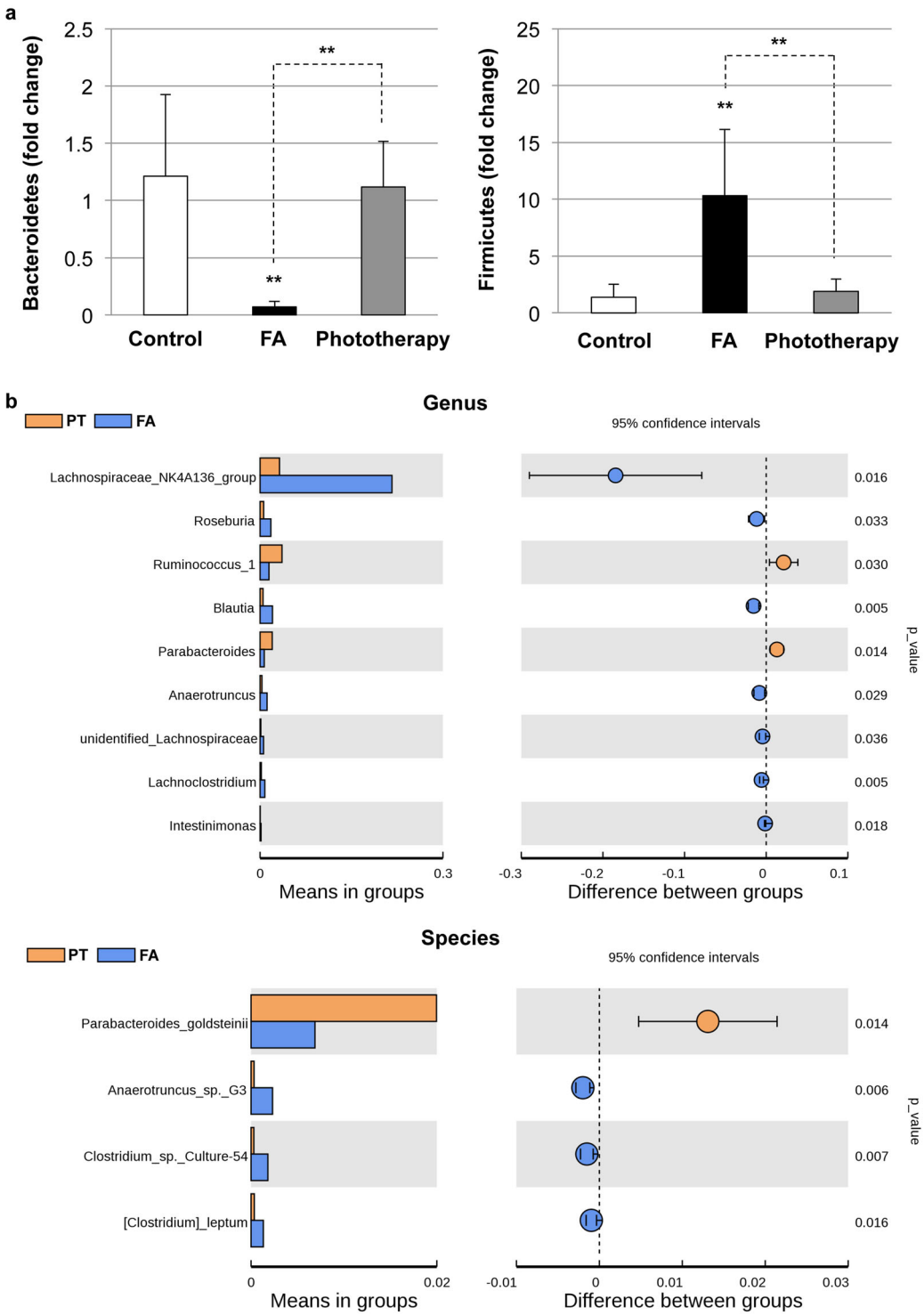

Fig. 6 Altered fecal microbiota composition in food allergy (FA). a Quantitative real-time PCR for verification of the phyla *Bacteroidetes* and *Firmicutes*. Values are presented as the mean ± SD of at least eight individuals in each group. $^{**}P < 0.01$ vs. the control or phototherapy group (Student's *t* test). **b** Beta diversity comparison of gut microbiomes between the FA and phototherapy groups. The data indicate the abundance of species and the difference between groups (95% confidential interval) at the genus and species levels. FA food allergy, PT phototherapy.

allergic response by endogenous vitamin D_3. Vitamin D_3-mediated activation of VDR and the subsequent induction of Nrf2-antioxidant signaling (Fig. 5) may play an important role in maintaining the integrity of the intestinal mucosal barrier[40], resulting in the amelioration of allergic diarrhea.

Another potential mechanism of phototherapy in the prevention of FA could be the modulation of gut microbiota (Fig. 6). In line with our current data, a recent study demonstrated the existence of a link between vitamin D_3 deficiency and altered gut microbiota composition characterized by the reduction in the phylum *Bacteroidetes* and the elevation of the phylum *Firmicutes*[41]. Interestingly, FA-associated dysbiosis could directly transfer FA symptoms in naïve BALB/c mice (Fig. 7), suggesting the existence of unique microbacteria in FA donor feces that can induce the

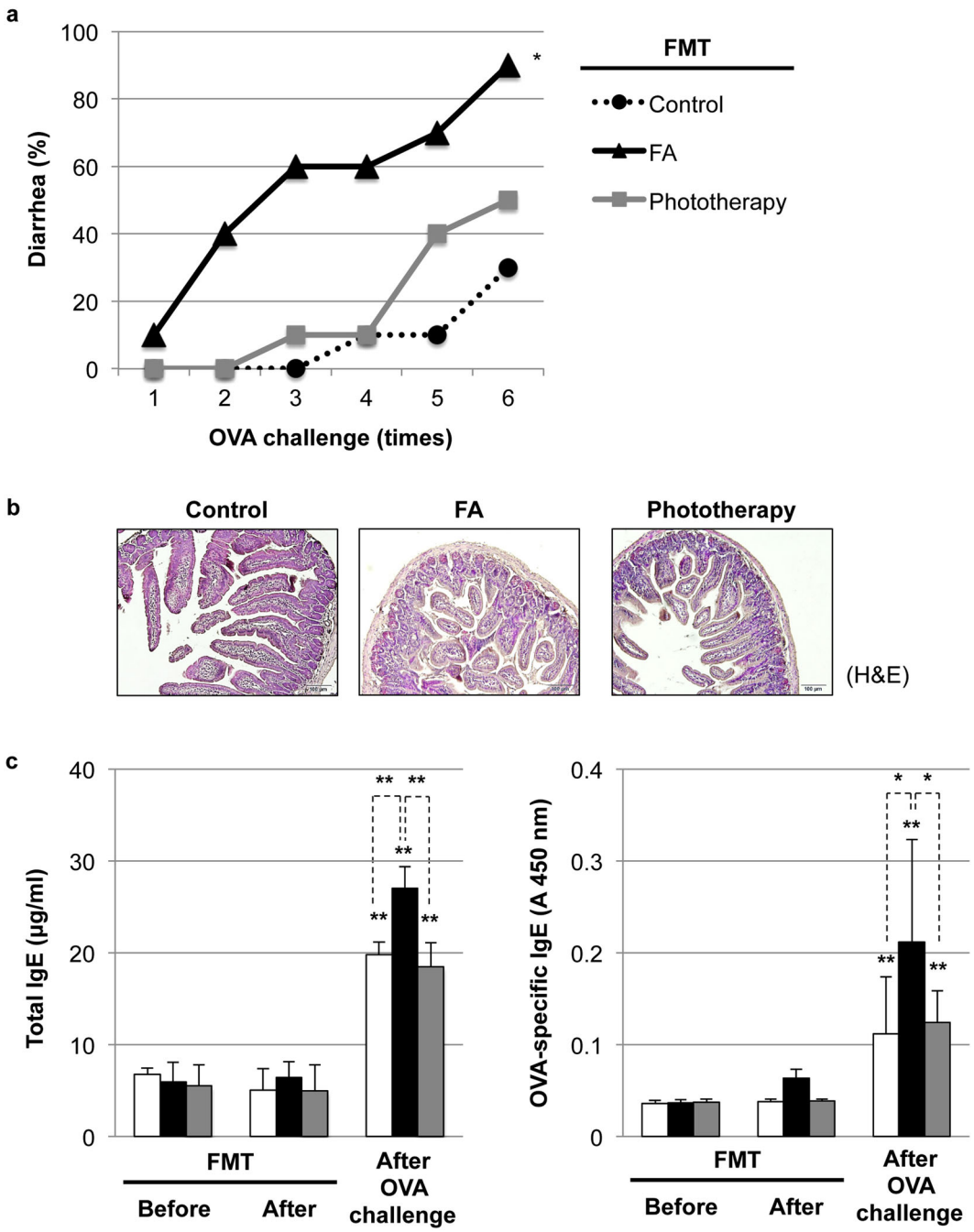

Fig. 7 Application of fecal microbiota transplantation (FMT) for functional evaluation of food allergy (FA)-associated dysbiosis. a The incidence of allergic diarrhea in naïve mice with FMT. After antibiotic-induced dysbiosis, a 200-μl/day aliquot of the resuspended material (5-mg/ml feces from control, FA or phototherapy group, $n = 10$ per group) was given by oral gavage for 3 days. Two weeks after FMT, repeated intragastric (i.g.) OVA challenge was performed, and allergic diarrhea was assessed visually by monitoring mice for 30 min after each i.g. exposure. *$P < 0.05$ vs. the control-FMT group (Tukey's multiple comparisons test). **b** Histological evaluation of the intestines of naïve mice with FMT after the 6th OVA challenge. The pictures at ×100 magnification are representative of ten individuals in each group. H&E hematoxylin and eosin staining. Scale bar: 100 μm. **c** Elevation of total and OVA-specific IgE after the 6th OVA challenge in FMT mice with donor FA feces (FA-FMT mice, black bar) as compared with the levels in control-FMT (white bar) or phototherapy-FMT (gray bar) mice. Values are presented as the mean ± SD of ten individuals in each group. *, **, $P < 0.05$ and 0.01 vs. baseline data before FMT or the indicated pair, respectively (Student's *t* test).

OVA-specific IgE response and subsequent allergic diarrhea. In this study, the genus *Lachnospiraceae_NK4A136_group* was identified as an FA-associated microbacteria. In concordance with our study, another study also mentioned the elevation of the *Lachnospiraceae_NK4A136_group* in patients with wheat-dependent exercise-induced anaphylaxis[42]. The replacement of FA-associated bacteria with healthy microbiota may be a promising strategy for FA therapeutics (Fig. 8). In addition, one of the beneficial bacterial species, *Parabacteroides goldsteinii* (phylum *Bacteroidetes*), was enriched in phototherapy-treated mice. Interestingly, *Parabacteroides goldsteinii* was enriched in the offspring of goat-milk-fed pregnant mice and may provide a protective effect against atopy

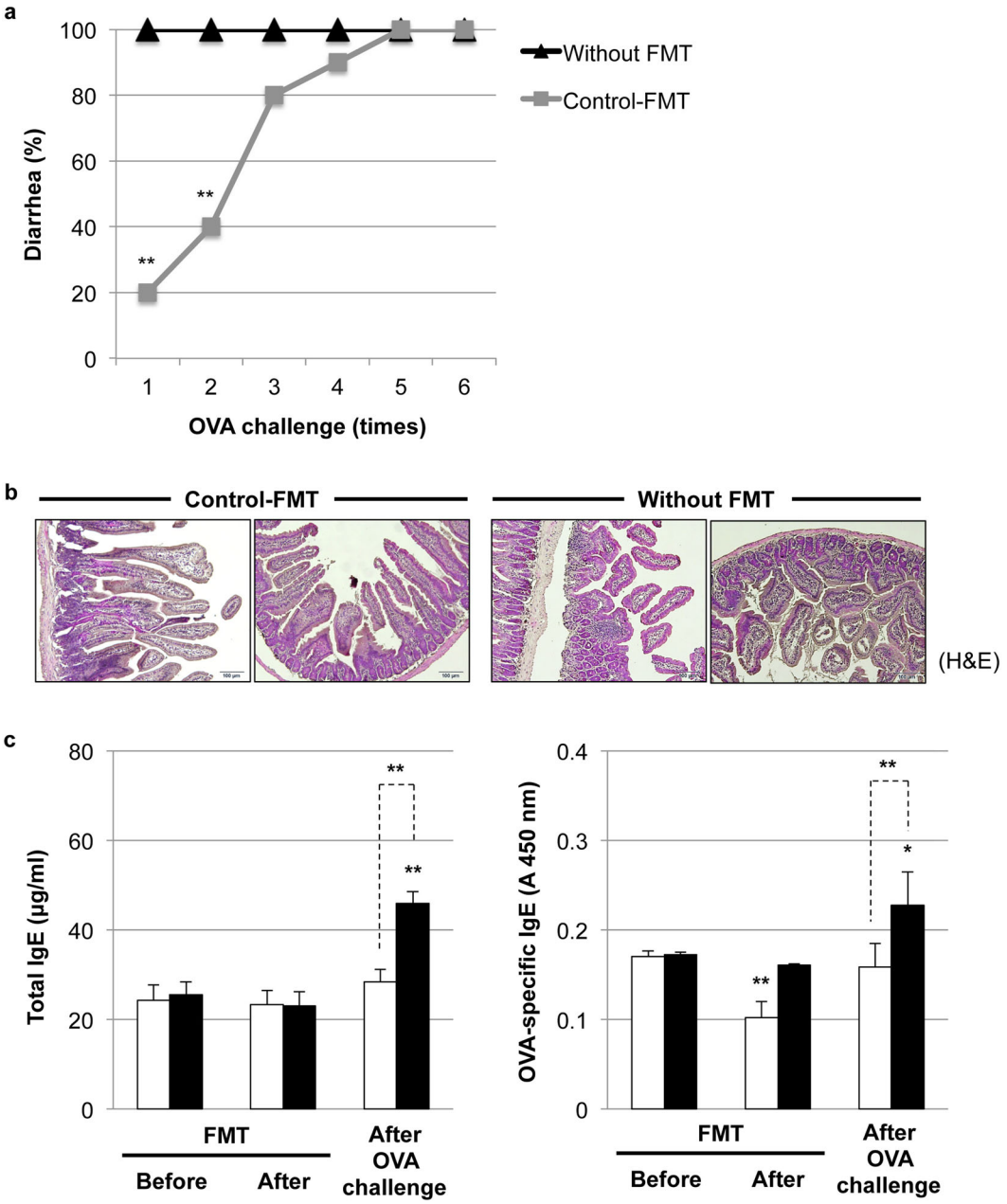

Fig. 8 Application of fecal microbiota transplantation (FMT) for the therapeutic modulation of diseased microbiota. a Therapeutic modulation of gut microbiota by FMT in FA mice. After the development of FA and following antibiotic-induced dysbiosis, FMT with control donor feces (control-FMT) was administered to FA mice ($n = 10$). FA mice without FMT ($n = 5$) were set as a comparison. Allergic diarrhea was assessed visually by monitoring mice for 30 min after each i.g. exposure. $^{**}P < 0.01$ vs. FA mice without FMT (Tukey's multiple comparisons test). **b** Histological evaluation of the intestines of FA mice with/without control-FMT after the 6th OVA challenge. The pictures at ×100 magnification are representative of ten individuals in each group. H&E hematoxylin and eosin staining. Scale bar: 100 μm. **c** Reduced expression of total and OVA-specific IgE after the 6th OVA challenge in FA mice with control-FMT (white bar). Black bar: FA mice without FMT. Values are presented as the mean ± SD of ten individuals in each group. *, **, $P < 0.05$ and 0.01 vs. FA mice before FMT or the indicated pair, respectively (Student's *t* test).

development and alleviate allergen-induced airway inflammation in offspring[43]. Further studies are necessary to understand the impact of these unique microbes on FA development and prevention.

There are several limitations in this study. First, our animal model[44] is recognized as a model for FAs but this model does not completely mimic FA symptoms such as IgE-mediated anaphylaxis[45]. We need to carefully evaluate the impact of phototherapy on other FA symptoms as well as adverse events caused by phototherapy before we proceed to clinical application. Second, the correlation between vitamin D_3 and microbiota composition was not fully clarified in this study. Although we have no data to reveal the direct impact of vitamin D_3 supplementation on gut microbiota composition, the replacement of gut microbiota by FMT could not alter the vitamin D_3 level (Supplementary Figs. 6 and 8). Vitamin D_3 and gut microbiota composition may be independent of each other. Vitamin D_3 may be important for gut homeostasis, but its expression may not be regulated by the gut microbiota composition.

In summary, we proposed phototherapy as an alternative approach for the prevention and treatment of FA-like allergic

diarrhea, and it may maintain circulating vitamin D_3 and healthy microbiota for the prevention of FA. There are several clinical trials exploring the effect of vitamin D supplementation in the prevention of FAs, while there is a lack of consistent data addressing the preventive ability of vitamin D supplementation for FAs[46]. Of note, a recent randomized controlled trial revealed that daily high-dose vitamin D supplementation (30 µg, 1200 IU) does not prevent allergic sensitization but rather increases the risk of milk allergy in infants[47]. How to find an optimal dose of vitamin D_3 for effective prevention of FAs is one of the important issues for reducing the risk of adverse effects. Although it is too early to make a conclusion, a better approach to the prevention of FAs could be the use of phototherapy due to the induction of endogenous vitamin D_3 production at an optimal concentration as well as the modulation of gut microbiota. The exposure time and duration of phototherapy should be further considered for future clinical applications.

METHODS

Mice

Female BALB/c mice, 4 weeks of age, were obtained from the National Laboratory Animal Breeding and Research Center (Taipei, Taiwan). All animals were maintained in specific pathogen-free animal facilities with water and commercial rodent food provided ad libitum. Our experimental design was reviewed and approved by the Institutional Animal Care and Use Committee (Approval No. 2018122119) of Kaohsiung Chang Gung Memorial Hospital.

Establishment of a FA model and phototherapy

We prepared OVA-induced FA mice according to a previously described protocol[44] with minor modifications (Supplementary Fig. 9a). Briefly, BALB/c mice ($n = 26$) were divided into two groups: the FA group ($n = 14$) and the phototherapy group ($n = 12$). The phototherapy group received daily exposure to full spectrum light (color temperature 5500 K, color rendition indexes >90; Chang Gung Biotechnology, Taipei, Taiwan) (12 h/day) throughout the entire experiment (9 weeks). The distance between the animals and the full spectrum light was kept at ~45 cm (Supplementary Fig. 9b). Both groups were intraperitoneally immunized twice with a precipitate (100 µl/mouse) of OVA (60 µg, Sigma-Aldrich, St Louis, MO, USA) and aluminum hydroxide (1 mg, Thermo Fisher Scientific Inc., Rockford, IL, USA). After the second immunization with a 2-week interval, repeated intragastric (i.g.) OVA challenge was performed 15 times (every 2–3 days, 15 mg in a final volume of 150 µl of PBS). Naïve mice ($n = 8$) without OVA immunization were treated with PBS as a control. Allergic diarrhea was assessed visually by monitoring mice for 30 min after each i.g. exposure. Experimental mice were sacrificed after the final OVA challenge, and intestinal tissues, blood, and stool samples were collected for histological and biochemical analyses.

Histological assessment of FA

Experimental mice were sacrificed after the final OVA challenge, and the intestinal specimens were embedded in paraffin. The paraffin sections (5 µm) were dewaxed and stained with H&E or toluidine blue for evaluation of inflammation and mast cell infiltration. At least six randomly chosen high-power fields (HPFs) of each section were examined to yield the mean number of mast cells per HPF in the intestine.

Immunohistochemistry

After peroxidase blocking, antigen retrieval and blocking, the slides were incubated with rat monoclonal antibody against Mcpt-1 (200× dilution; Thermo Fisher Scientific Inc.), mouse monoclonal antibody against IL-25 (500× dilution; Thermo Fisher Scientific Inc.), mouse monoclonal antibody against IL-33 (200× dilution; Thermo Fisher Scientific Inc.), rabbit polyclonal antibody against TSLP (400× dilution; Thermo Fisher Scientific Inc.), rabbit polyclonal antibody against CYP27A1 (500× dilution; Thermo Fisher Scientific Inc.), or rabbit polyclonal antibody against CYP27B1 (500× dilution; Thermo Fisher Scientific Inc.) overnight at 4 °C followed by incubation with Rat or Mouse/Rabbit Probe HRP (BioTnA, Kaohsiung, Taiwan) for 30 min. After washing, chromogen development was performed by 3,3′-diaminobenzidine staining. Counter staining was carried out using hematoxylin. The slides were rinsed with H_2O and covered with resin-based mounting medium (BioTnA) after dehydration.

Total and OVA-specific immunoglobulins

The serum levels of total and OVA-specific IgG1, IgG2a, and IgE were determined by ELISA[48]. For evaluation of total immunoglobulin levels, anti-mouse IgG1, IgG2a, or IgE (250× dilution; BD Biosciences, San Jose, CA, USA) was coated onto 96-well microplates (Nalgene Nunc International, Roskilde, Denmark) and incubated overnight at 4 °C. For evaluation of OVA-specific immunoglobulin levels, OVA solution (50 mg/ml) was coated instead. After blocking, serum samples with appropriate dilution (total IgG1; 10,000× dilution, total IgG2a; 2000× dilution, total IgE; 250× dilution, OVA-specific IgG1; 2,000,000× dilution, OVA-specific IgG2a; 200,000× dilution, OVA-specific IgE; 10× dilution) were added to each well and incubated for 2 h at 37 °C. After washing, biotin-conjugated anti-mouse IgG1, IgG2a, or IgE (250× dilution; BD Biosciences) were added and incubated for 1.5 h at 37 °C followed by incubation with streptavidin-HRP (200× dilution; R&D Systems, Minneapolis, MN, USA) for 1 h. After washing, 1-Step Ultra TMB Substrate Solution (Thermo Fisher Scientific Inc.) was added for color development. After the addition of stop solution, the absorbance at 450 nm was measured using a Victor X4 Multilabel Plate Reader (PerkinElmer, Waltham, MA, USA).

RNA extraction and quantitative real-time PCR analysis

RNA was extracted from the mouse intestine using TRIzol (Thermo Fisher Scientific Inc.) and reverse transcribed with a High-Capacity cDNA Reverse Transcription Kit (Thermo Fisher Scientific Inc.). The expression levels of IL-25, IL-33, TSLP, VDR, CYP27A1, CYP27B1, Nrf2, HO-1, SOD1, and SOD2 were quantified using quantitative real-time PCR (Applied Biosystems, Foster, CA, USA) with specific primer sets as shown in Supplementary Table 1. β-Actin was used as an internal control for normalization.

Vitamin D_3 ELISA

The serum level of the active form of vitamin D_3 was measured using a General 1,25-Dihydroxyvitamin D_3 (DHVD3) ELISA Kit (MyBioSource, Inc., San Diego, CA, USA). Briefly, 50 µl of standard and serum samples (undiluted) were added to pre-coated plate with DHVD3 monoclonal antibody, and biotin-labeled DHVD3 analogs were immediately added for the competitive inhibition reaction. After incubation for 1 h at 37 °C, unbound conjugate was washed off followed by incubation with avidin-conjugated HRP (100 µl) for 30 min at 37 °C. After washing and addition of substrate solution (90 µl) for 15 min at 37 °C, stop solution (50 µl) was added and the absorbance at 450 nm was determined using a Victor X4 Multilabel Plate Reader (PerkinElmer).

Stool sample preparation, 16S ribosomal RNA gene amplicon sequencing, and fecal microbiota analysis

Stool samples were snap-frozen in liquid nitrogen before storage at −80 °C. Fecal DNA isolation, 16S rRNA gene amplicon sequencing and data analysis were performed by BIOTOOLS Co., Ltd., (New Taipei, Taiwan). Briefly, total genomic DNA was extracted using the CTAB/SDS method, and DNA was diluted to 1 ng/µl using sterile water. For 16S rRNA sequencing, the V4 region was amplified with a specific primer (515F-806R). All PCRs were carried out with Phusion® High-Fidelity PCR Master Mix (New England Biolabs, Ipswitch, MA, USA). The PCR products were monitored on a 2% agarose gel, and samples with bright main strips between 400 and 450 bp were chosen and purified with a Qiagen Gel Extraction Kit (Qiagen, Hilden, Germany). Sequencing libraries were generated using the NEBNext® Ultra™ DNA Library Pre Kit for Illumina® (New England Biolabs) following the manufacturer's recommendations, and index codes were added. The library was sequenced on an Illumina platform (Illumina, San Diego, CA, USA), and 250-bp paired-end reads were generated. Paired-end reads were assigned to samples based on their unique barcode and truncated by cutting off the barcode and primer sequence. Paired-end reads were merged using FLASH (V1.2.7, http://ccb.jhu.edu/software/FLASH/), and the splicing sequences were called raw tags. Quality filtering of the raw tags was performed under specific filtering conditions to obtain the high-quality clean tags according to the QIIME quality control process (V1.7.0, http://qiime.org/index.html). The tags were compared with the reference database (Gold database, http://drive5.com/uchime/uchime_download.html) using the UCHIME algorithm (http://www.drive5.com/usearch/

manual/uchime_algo.html) to detect chimera sequences (http://www.drive5.com/usearch/manual/chimera_formation.html). Then, the chimera sequences were removed to obtain effective tags.

For fecal microbiota analysis, alpha and beta diversity were determined based on output normalized data with QIIME software (V1.7.0). LEfSe analysis was performed to determine most abundant taxa among groups. A histogram of LDA scores is shown as the result of LEfSe analysis. LDA scores larger than 4 were displayed in the final output. A *t*-test was performed to determine species with significant variation between groups at various taxon ranks, including phylum, class, order, family, genus, and species.

Quantitative real-time PCR analysis for bacterial DNA

Fecal bacterial DNA was extracted from the stool using a QIAamp Fast DNA Stool Mini Kit (Qiagen), and the expression levels of *Bacteroidetes* and *Firmicutes* were quantified using quantitative real-time PCR (Applied Biosystems) with specific primer sets as shown in Supplementary Table 2[49]. Total bacteria were used as an endogenous control to normalize gene expression.

FMT

To explore the impact of FA-associated dysbiosis on FA symptoms, FMT was conducted on naïve mice. Before conducting FMT, naïve BALB/c mice ($n = 30$) received therapeutic-dose ampicillin (500 mg/kg) by oral gavage for 14 consecutive days[50] with ampicillin (1 g/l) in drinking water ad libitum[51] for antibiotic-induced gut dysbiosis. Then, a 200-µl/day aliquot of the resuspended material (5-mg/ml feces from the control, FA or phototherapy group, $n = 10$ per group) was given by oral gavage for 3 days[51]. To explore the therapeutic potential of FMT for the modulation of FA-associated dysbiosis, established FA mice ($n = 10$) received antibiotic-induced gut dysbiosis followed by FMT with donor control feces. The microbiota composition before and after FMT was evaluated by quantitative real-time PCR analysis. Two weeks after FMT, OVA challenge was performed and FA symptoms were evaluated as described above.

Statistical analysis

Unpaired two-tailed Student's *t* test was used to determine the significance of the difference between normally distributed means of the expression ratio in two groups. Tukey's multiple comparisons test was used to determine the significance of the difference between each pair of means with appropriate adjustment for multiple testing. Each sample was tested in triplicate, and the results are indicated as the mean ± SD. Statistical analysis was performed using SPSS software version 22 (IBM, Armonk, NY, USA) or GraphPad Prism 7 software (GraphPad Software, La Jolla, CA, USA). A value of $P < 0.05$ was considered to be significant.

Reporting summary

Further information on research design is available in the Nature Research Reporting Summary linked to this article.

DATA AVAILABILITY

Raw data from the fecal microbiota analysis are deposited in the SRA database public repository from NCBI within the Bioproject accession number PRJNA690991.

Received: 12 October 2020; Accepted: 18 March 2021;
Published online: 06 May 2021

REFERENCES

1. Comberiati, P. et al. Diagnosis and treatment of pediatric food allergy: an update. *Ital. J. Pediatr.* **41**, 13 (2015).
2. Devdas, J. M., McKie, C., Fox, A. T. & Ratageri, V. H. Food allergy in children: an overview. *Indian J. Pediatr.* **85**, 369–374 (2018).
3. Gupta, R. S. et al. Hygiene factors associated with childhood food allergy and asthma. *Allergy Asthma Proc.* **37**, e140–e146 (2016).
4. Poulsen, L. K. Allergy assessment of foods or ingredients derived from biotechnology, gene-modified organisms, or novel foods. *Mol. Nutr. Food Res.* **48**, 413–423 (2004).
5. Shahali, Y. & Dadar, M. Plant food allergy: influence of chemicals on plant allergens. *Food Chem. Toxicol.* **115**, 365–374 (2018).
6. Potaczek, D. P. et al. Epigenetics and allergy: from basic mechanisms to clinical applications. *Epigenomics* **9**, 539–571 (2017).
7. Du Toit, G. et al. Randomized trial of peanut consumption in infants at risk for peanut allergy. *N. Engl. J. Med.* **372**, 803–813 (2015).
8. Rudders, S. A. & Camargo, C. A. Jr. Sunlight, vitamin D and food allergy. *Curr. Opin. Allergy Clin. Immunol.* **15**, 350–357 (2015).
9. Camargo, C. A. Jr., Clark, S., Kaplan, M. S., Lieberman, P. & Wood, R. A. Regional differences in EpiPen prescriptions in the United States: the potential role of vitamin D. *J. Allergy Clin. Immunol.* **120**, 131–136 (2007).
10. Mullins, R. J. & Camargo, C. A. Latitude, sunlight, vitamin D, and childhood food allergy/anaphylaxis. *Curr. Allergy Asthma Rep.* **12**, 64–71 (2012).
11. Matsui, T. et al. Sun exposure inversely related to food sensitization during infancy. *Pediatr. Allergy Immunol.* **26**, 628–633 (2015).
12. Tanaka, K. et al. The relationship between the season of birth and early-onset food allergies in children. *Pediatr. Allergy Immunol.* **26**, 607–613 (2015).
13. Norval, M. et al. The human health effects of ozone depletion and interactions with climate change. *Photochem. Photobiol. Sci.* **10**, 199–225 (2011).
14. Gordon, J. R. & Brieva, J. C. Images in clinical medicine. Unilateral dermatoheliosis. *N. Engl. J. Med.* **366**, e25 (2012).
15. Hoel, D. G. & de Gruijl, F. R. Sun exposure public health directives. *Int. J. Environ. Res. Public Health* **15**, 2794 (2018).
16. Grzybowski, A. & Pietrzak, K. From patient to discoverer—Niels Ryberg Finsen (1860–1904)—the founder of phototherapy in dermatology. *Clin. Dermatol.* **30**, 451–455 (2012).
17. Stumpf, W. E. & Privette, T. H. Light, vitamin D and psychiatry. Role of 1,25 dihydroxyvitamin D3 (soltriol) in etiology and therapy of seasonal affective disorder and other mental processes. *Psychopharmacology* **97**, 285–294 (1989).
18. Tseng, P. T. et al. Light therapy in the treatment of patients with bipolar depression: a meta-analytic study. *Eur. Neuropsychopharmacol.* **26**, 1037–1047 (2016).
19. Jurvelin, H., Jokelainen, J. & Takala, T. Transcranial bright light and symptoms of jet lag: a randomized, placebo-controlled trial. *Aerosp. Med. Hum. Perform.* **86**, 344–350 (2015).
20. van Maanen, A., Meijer, A. M., van der Heijden, K. B. & Oort, F. J. The effects of light therapy on sleep problems: a systematic review and meta-analysis. *Sleep. Med. Rev.* **29**, 52–62 (2016).
21. Aarts, M. P., Aries, M. B., Diakoumis, A. & van Hoof, J. Shedding a light on phototherapy studies with people having dementia: a critical review of the methodology from a light perspective. *Am. J. Alzheimer's Dis. Other Dement.* **31**, 551–563 (2016).
22. Figueiro, M. G. Light, sleep and circadian rhythms in older adults with Alzheimer's disease and related dementias. *Neurodegener. Dis. Manag.* **7**, 119–145 (2017).
23. Stokowski, L. A. Fundamentals of phototherapy for neonatal jaundice. *Adv. Neonatal Care* **6**, 303–312 (2006).
24. Nakano, T. et al. Impact of artificial sunlight therapy on the progress of non-alcoholic fatty liver disease in rats. *J. Hepatol.* **55**, 415–425 (2011).
25. Geier, A. et al. Treatment of non-alcoholic steatohepatitis patients with vitamin D: a double-blinded, randomized, placebo-controlled pilot study. *Scand. J. Gastroenterol.* **53**, 1114–1120 (2018).
26. Goto, S. et al. Application of artificial sunlight for the elderly as a possible environmental nursing practice. *POJ Nurs. Pract. Res.* **2**, 1–5, https://proskolar.org/wp-content/uploads/2018/02/Application-of-Artificial-Sunlight-for-the-Elderly-as-a-Possible-Environmental-Nursing-Practice.pdf (2018).
27. Hiratsuka, T. et al. Phototherapy with artificial light suppresses dextran sulfate sodium-induced colitis in a mouse model. *J. Gastroenterol. Hepatol.* **29**, 749–756 (2014).
28. Hara, T. et al. Intraperitoneal phototherapy suppresses inflammatory reactions in a surgical model of peritonitis. *J. Surg. Res.* **252**, 231–239 (2020).
29. Shu, S. A. et al. Microbiota and food allergy. *Clin. Rev. Allergy Immunol.* **57**, 83–97 (2019).
30. Zhao, W., Ho, H. E. & Bunyavanich, S. The gut microbiome in food allergy. *Ann. Allergy Asthma Immunol.* **122**, 276–282 (2019).
31. Bunyavanich, S. & Berin, M. C. Food allergy and the microbiome: current understandings and future directions. *J. Allergy Clin. Immunol.* **144**, 1468–1477 (2019).
32. Aitoro, R. et al. Gut microbiota as a target for preventive and therapeutic intervention against food allergy. *Nutrients* **9**, 672 (2017).
33. Kang, Y. & Cai, Y. Future prospect of faecal microbiota transplantation as a potential therapy in asthma. *Allergologia et. Immunopathologia* **46**, 307–309 (2018).
34. Malaguarnera, L. Vitamin D and microbiota: two sides of the same coin in the immunomodulatory aspects. *Int. Immunopharmacol.* **79**, 106112 (2020).
35. Bosman, E. S., Albert, A. Y., Lui, H., Dutz, J. P. & Vallance, B. A. Skin exposure to narrow band ultraviolet (UVB) light modulates the human intestinal microbiome. *Front. Microbiol.* **10**, 2410 (2019).
36. Khodoun, M. V., Tomar, S., Tocker, J. E., Wang, Y. H. & Finkelman, F. D. Prevention of food allergy development and suppression of established food allergy by

neutralization of thymic stromal lymphopoietin, IL-25, and IL-33. *J. Allergy Clin. Immunol.* **141**, 171–179.e1 (2018).
37. Antunes, M. M. et al. Oral supplementation with capsaicin reduces oxidative stress and IL-33 on a food allergy murine model. *World Allergy Organ. J.* **12**, 100045 (2019).
38. Ling, Z. et al. Altered fecal microbiota composition associated with food allergy in infants. *Appl. Environ. Microbiol.* **80**, 2546–2554 (2014).
39. Lindner, J. et al. Endogenous calcitriol synthesis controls the humoral IgE response in mice. *J. Immunol.* **199**, 3952–3958 (2017).
40. Yao, B. et al. The protective effect of lithocholic acid on the intestinal epithelial barrier is mediated by the vitamin D receptor via a SIRT1/Nrf2 and NF-kappaB dependent mechanism in Caco-2 cells. *Toxicol. Lett.* **316**, 109–118 (2019).
41. Guida, F. et al. Altered gut microbiota and endocannabinoid system tone in vitamin D deficiency-mediated chronic pain. *Brain, Behav., Immun.* **85**, 128–141 (2020).
42. Du, Z., Gao, X. & Yin, J. Gut microbiome alterations in patients with wheat-dependent exercise-induced anaphylaxis. *Int. Immunopharmacol.* **84**, 106557 (2020).
43. Kao, H. F. et al. Goat milk consumption enhances innate and adaptive immunities and alleviates allergen-induced airway inflammation in offspring mice. *Front. Immunol.* **11**, 184 (2020).
44. Golias, J. et al. Heat-induced structural changes affect OVA-antigen processing and reduce allergic response in mouse model of food allergy. *PLoS ONE* **7**, e37156 (2012).
45. Brandt, E. B. et al. Mast cells are required for experimental oral allergen-induced diarrhea. *J. Clin. Investig.* **112**, 1666–1677 (2003).
46. Peroni, D. G. & Boner, A. L. Food allergy: the perspectives of prevention using vitamin D. *Curr. Opin. Allergy Clin. Immunol.* **13**, 287–292 (2013).
47. Rosendahl, J. et al. High-dose vitamin D supplementation does not prevent allergic sensitization of infants. *J. Pediatrics* **209**, 139–145.e1 (2019).
48. Nakano, T. et al. Impact of histone H1 on the progression of allergic rhinitis and its suppression by neutralizing antibody in mice. *PLoS ONE* **11**, e0153630 (2016).
49. Anitha, M. et al. Intestinal dysbiosis contributes to the delayed gastrointestinal transit in high-fat diet fed mice. *Cell. Mol. Gastroenterol. Hepatol.* **2**, 328–339 (2016).
50. Shi, Y. et al. Structural and functional alterations in the microbial community and immunological consequences in a mouse model of antibiotic-induced dysbiosis. *Front. Microbiol.* **9**, 1948 (2018).
51. Le Bastard, Q. et al. Fecal microbiota transplantation reverses antibiotic and chemotherapy-induced gut dysbiosis in mice. *Sci. Rep.* **8**, 6219 (2018).

ACKNOWLEDGEMENTS

This work was supported in part by grants from the Ministry of Science and Technology (MOST106-2320-B-182-033, MOST107-2320-B-182-032, and MOST109-2320-B-182-014 to T.N.) and Chang Gung Medical Foundation (CMRPD8C0562, CMRPD8D1381, CMRPD8F0911, CMRPD8F0912, CMRPD8I0011, and CMRPD8I0012 to T.N.). The founders had no role in the study design, data collection and analysis, decision to publish, or preparation of the manuscript.

AUTHOR CONTRIBUTIONS

P.-J.C. and T.N. contributed equally to this manuscript. T.N. designed and supervised the experiments; P.-J.C., C.-Y.L., and K.-C.C. performed the experiments and generated figures; T.N. and C.-L.C. provided research resources and contributed funding acquisition; T.N. and S.G. discussed the results; P.-J.C. and T.N. wrote the original draft; and T.N., K.-C.C. and S.G. reviewed and edited the draft.

COMPETING INTERESTS

The authors declare no competing interests.

ADDITIONAL INFORMATION

Supplementary information The online version contains supplementary material available at https://doi.org/10.1038/s41522-021-00213-8.

Correspondence and requests for materials should be addressed to T.N.

Reprints and permission information is available at http://www.nature.com/reprints

Publisher's note Springer Nature remains neutral with regard to jurisdictional claims in published maps and institutional affiliations.

Open Access This article is licensed under a Creative Commons Attribution 4.0 International License, which permits use, sharing, adaptation, distribution and reproduction in any medium or format, as long as you give appropriate credit to the original author(s) and the source, provide a link to the Creative Commons license, and indicate if changes were made. The images or other third party material in this article are included in the article's Creative Commons license, unless indicated otherwise in a credit line to the material. If material is not included in the article's Creative Commons license and your intended use is not permitted by statutory regulation or exceeds the permitted use, you will need to obtain permission directly from the copyright holder. To view a copy of this license, visit http://creativecommons.org/licenses/by/4.0/.

© The Author(s) 2021

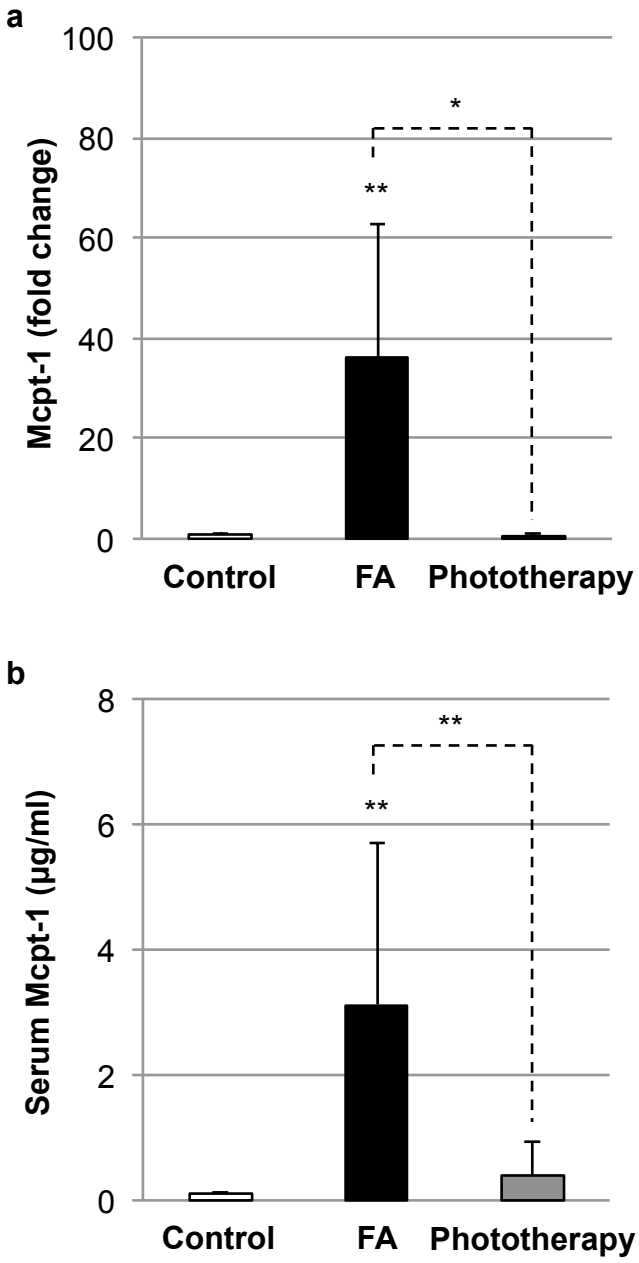

Supplementary Figure 1. The elevation of mast cell protease 1 (Mcpt-1) in food allergy (FA). FA-associated mucosal mast cell activation in the intestine (a) and the circulating level of Mcpt-1 (b) were evaluated by quantitative real-time PCR and ELISA, respectively. Values are presented as the mean ± SD of at least eight individuals in each group. *, **, $P < 0.05$ and 0.01 *vs.* FA mice, respectively (Student's *t*-test).

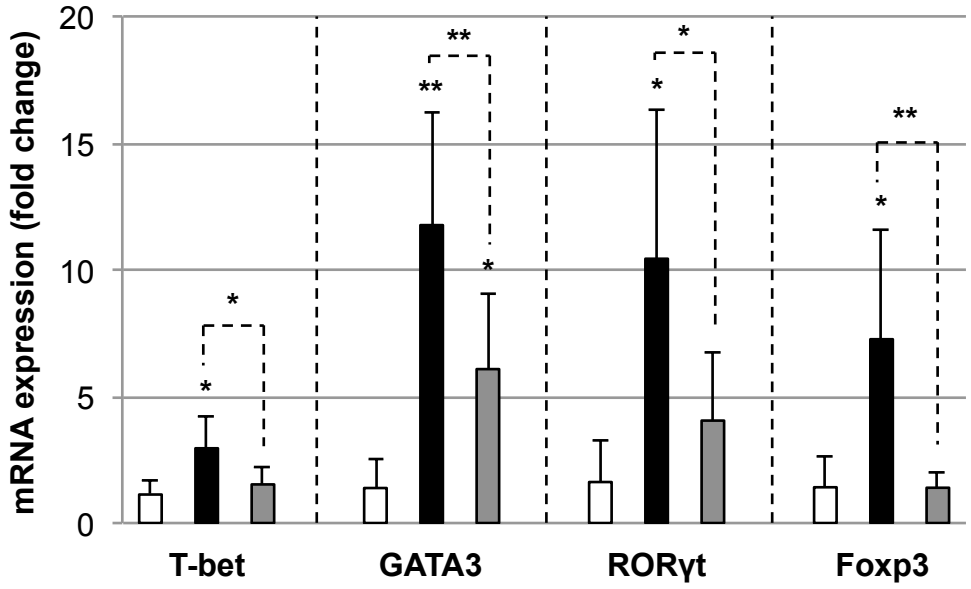

Supplementary Figure 2. Impact of phototherapy on T cell phenotypes. Intestinal levels of T-bet (Th1), GATA3 (Th2), RoRγt (Th17) and Foxp3 (regulatory T cells, Treg) were determined by quantitative real-time PCR analysis. Values are presented as the mean ± SD of at least eight individuals in each group. White bar: control, black bar: FA, gray bar: phototherapy. *, **, $P < 0.05$ and 0.01 *vs.* the control group, respectively (Student's *t*-test).

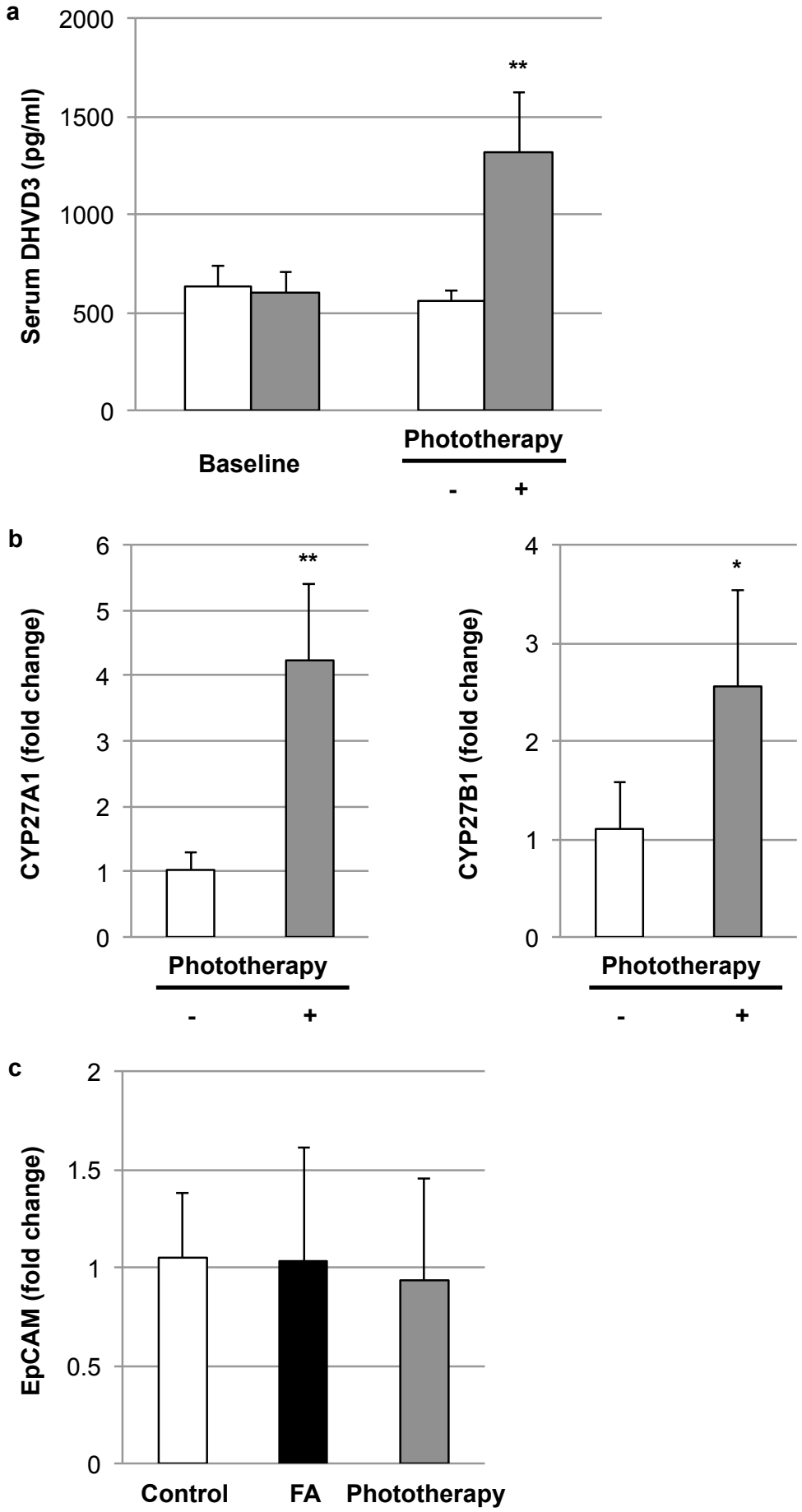
a
Serum DHVD3 (pg/ml)
2000
1500
1000
500
0
**
Baseline
Phototherapy
-
+
b
CYP27A1 (fold change)
6
5
4
3
2
1
0
**
Phototherapy
-
+
CYP27B1 (fold change)
4
3
2
1
0
*
Phototherapy
-
+
c
EpCAM (fold change)
2
1.5
1
0.5
0
Control
FA
Phototherapy

Supplementary Figure 3. Impact of phototherapy on vitamin D_3 metabolism in naïve mice. (a) Serum levels of vitamin D_3 were measured by ELISA. Values are presented as the mean ± SD of five individuals in each group. **, $P < 0.01$ (Student's *t*-test) *vs.* the control group. (b) Intestinal levels of sterol 27-hydroxylase (CYP27A1) and 25-hydroxyvitamin D_3-1α hydroxylase (CYP27B1) were evaluated by quantitative real-time PCR. Values are presented as the mean ± SD of five individuals in each group. *, **, $P < 0.05$ and 0.01 *vs.* the control group, respectively (Student's *t*-test). (c) The expression profiles of epithelial cell adhesion molecule (EpCAM) in the control, food allergy (FA) and phototherapy groups were evaluated by quantitative real-time PCR.

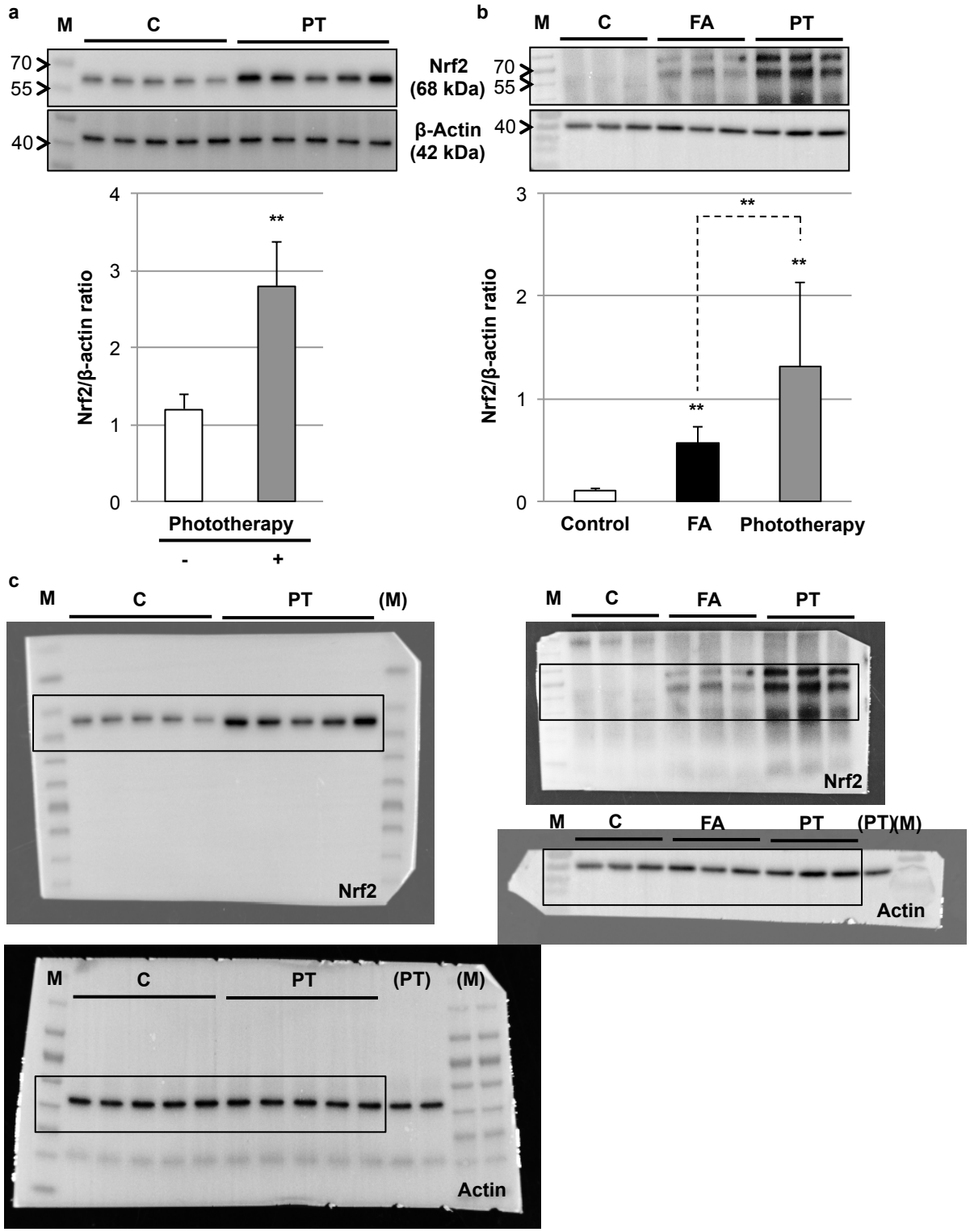
a
M
C
PT
70
55
40
Nrf2/β-actin ratio
Phototherapy
-
+
b
M
C
FA
PT
Nrf2
(68 kDa)
β-Actin
(42 kDa)
Control
FA
Phototherapy
c
(M)
Nrf2
Actin
(PT)

Supplementary Figure 4. Impact of phototherapy on intestinal nuclear factor erythroid 2-related factor 2 (Nrf2) expression in naïve and food allergy (FA) mice. (a) Phototherapy for 9 weeks significantly enhanced the intestinal Nrf2 expression. Values are presented as the mean ± SD of five individuals in each group. **, $P < 0.01$ *vs.* the control group (Student's *t*-test). (b) FA induced intestinal Nrf2 expression, and its expression was further enhanced by phototherapy. The blot data are representative of three independent experiments. They are derived from the same experiment and processed in parallel. M: molecular weight marker, C: control, FA: food allergy, PT: phototherapy. Values are presented as the mean ± SD of three individuals in each group. **, $P < 0.01$ *vs.* the control or phototherapy group (Student's *t*-test). (c) Full, un-cropped images of all blots. Some blot data include additional samples or molecular weight markers, which are excluded in the cropped image (a and b).

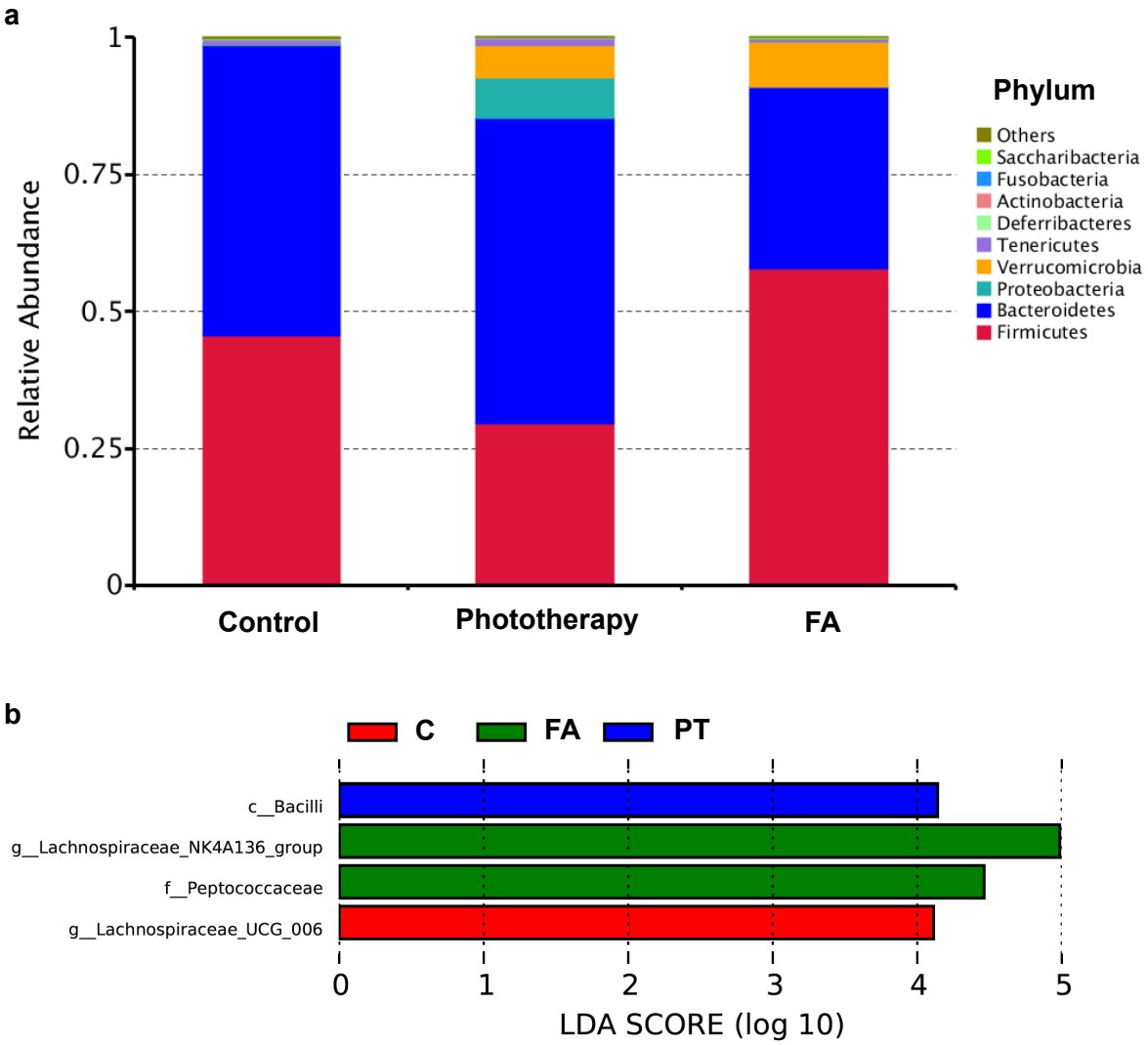

Supplementary Figure 5. Fecal microbiota composition. (a) Bacterial phyla in the control, FA and phototherapy groups (n=3 in each group). (b) Linear discriminant analysis (LDA) effect size (LEfSe) analysis was performed to determine the most abundant taxa among groups. Only genera with LDA scores greater than 4 are displayed. C: control, FA: food allergy, PT: phototherapy.

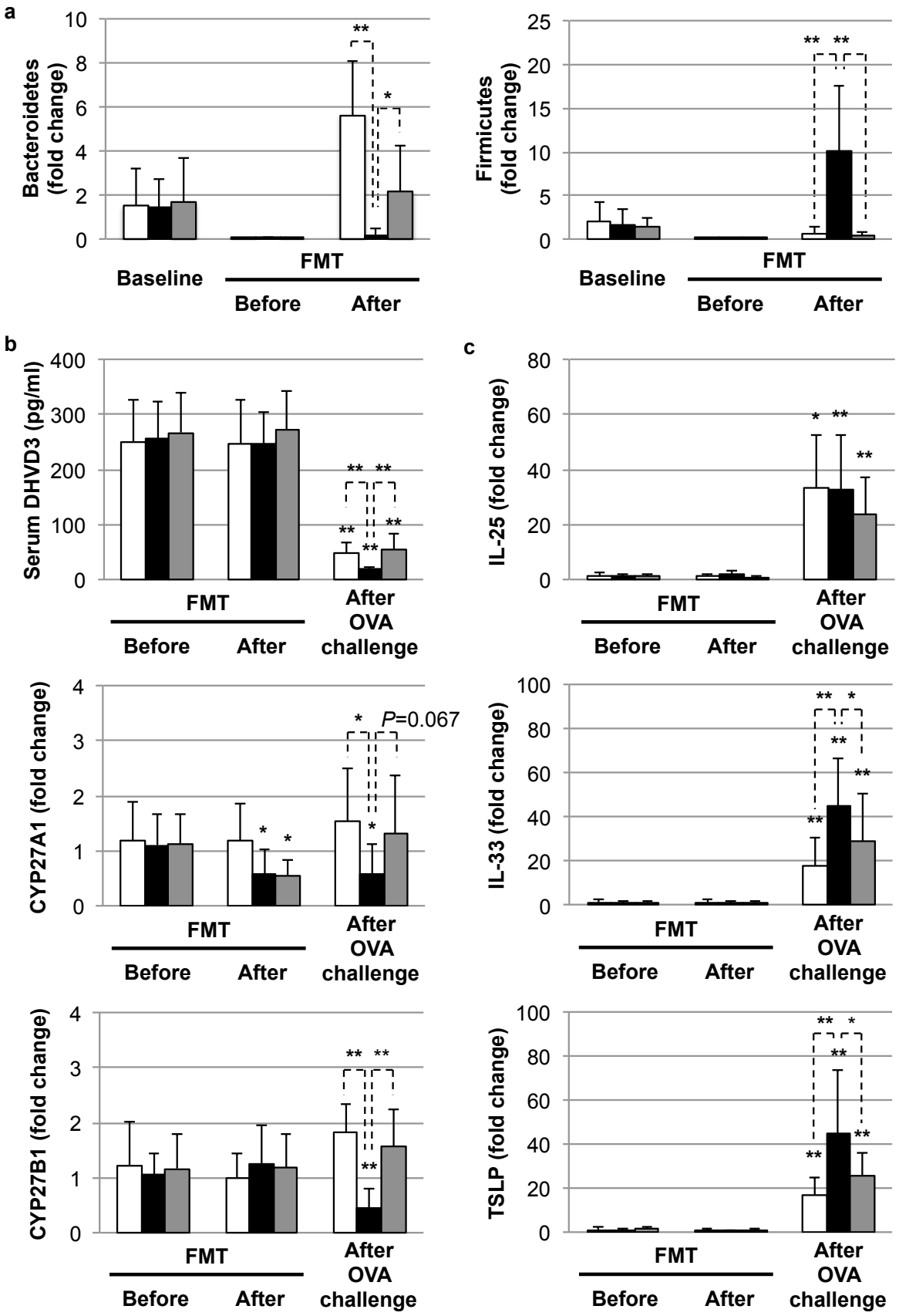
a
Bacteroidetes (fold change)
Baseline
FMT
Before
After
Firmicutes (fold change)
b
Serum DHVD3 (pg/ml)
After OVA challenge
c
IL-25 (fold change)
CYP27A1 (fold change)
P=0.067
IL-33 (fold change)
CYP27B1 (fold change)
TSLP (fold change)

Supplementary Figure 6. Impact of fecal microbiota transplantation (FMT) on the fecal microbiota composition, vitamin D_3 metabolism and intestinal cytokine expression in naïve mice. (a) Naïve BALB/c mice received FMT with control donor feces (control-FMT, white bar, n=10), food allergy (FA) donor feces (FA-FMT, black bar, n=10) or phototherapy donor feces (phototherapy-FMT, gray bar, n=10). The phyla *Bacteroidetes* and *Firmicutes* were evaluated by quantitative real-time PCR. *, **, $P< 0.05$ and 0.01, respectively (Student's *t*-test). (b) Serum levels of vitamin D_3 or intestinal levels of sterol 27-hydroxylase (CYP27A1) and 25-hydroxyvitamin D_3-1α hydroxylase (CYP27B1) were evaluated by ELISA and quantitative real-time PCR, respectively. *, **, $P< 0.05$ and 0.01 *vs.* baseline or the indicated pair, respectively (Student's *t*-test). (c) Intestinal levels of IL-25, IL-33 and thymic stromal lymphopoietin (TSLP) were evaluated by quantitative real-time PCR. *, **, $P< 0.05$ and 0.01 *vs.* baseline or the indicated pair, respectively (Student's *t*-test).

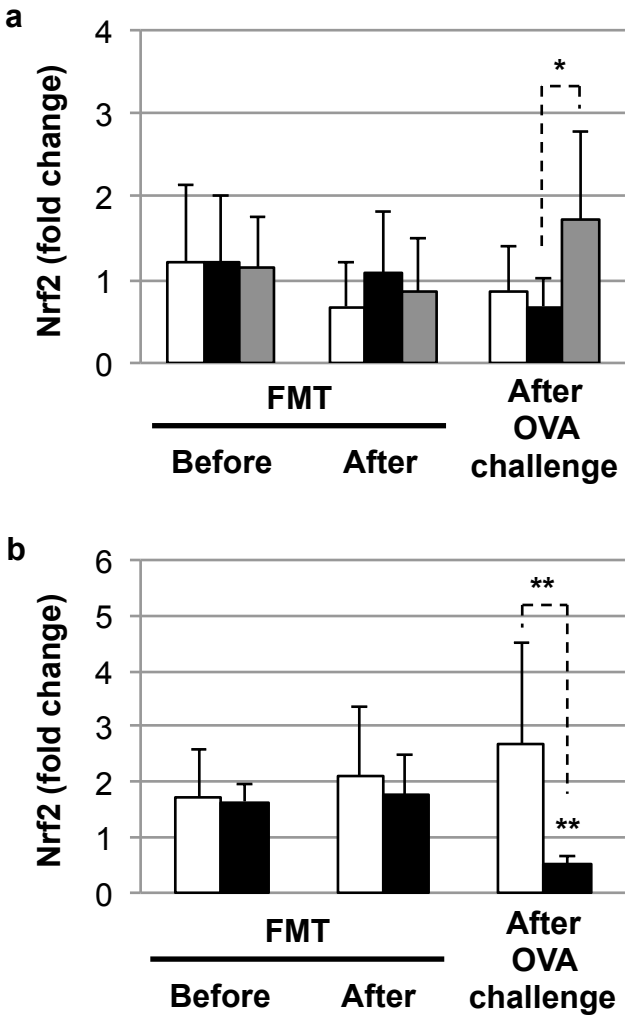

Supplementary Figure 7. Impact of fecal microbiota transplantation (FMT) on oxidative stress response in naïve and food allergy (FA) mice. (a) Naïve BALB/c mice received FMT with control donor feces (control-FMT, white bar, n=10), food allergy (FA) donor feces (FA-FMT, black bar, n=10) or phototherapy donor feces (phototherapy-FMT, gray bar, n=10). (b) FA mice received FMT with control donor feces (control-FMT, white bar, n=10). FA mice without FMT (black bar, n=5) were set as a comparison. Intestinal level of nuclear factor erythroid 2-related factor 2 (Nrf2) was evaluated by quantitative real-time PCR. *, **, $P < 0.05$ and 0.01 *vs.* baseline or the indicated pair, respectively (Student's *t*-test).

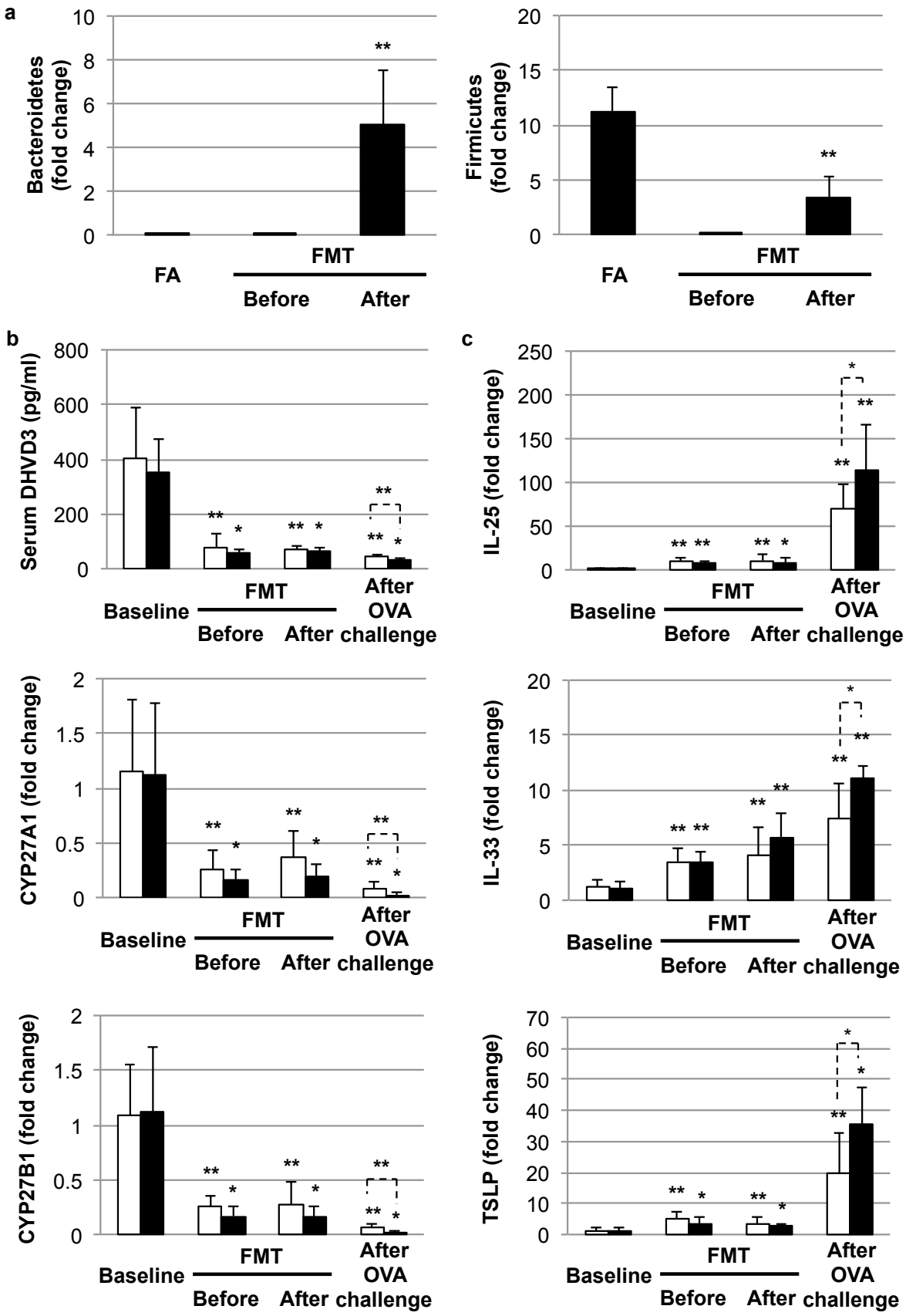
a
Bacteroidetes (fold change)
10
8
6
4
2
0
**
FA
FMT
Before
After
Firmicutes (fold change)
20
15
10
5
0
**
FA
FMT
Before
After
b
Serum DHVD3 (pg/ml)
800
600
400
200
0
Baseline
FMT
Before
After
After OVA challenge
c
IL-25 (fold change)
250
200
150
100
50
0
CYP27A1 (fold change)
2
1.5
1
0.5
0
IL-33 (fold change)
20
15
10
5
0
CYP27B1 (fold change)
2
1.5
1
0.5
0
TSLP (fold change)
70
60
50
40
30
20
10
0

Supplementary Figure 8. Impact of fecal microbiota transplantation (FMT) on the fecal microbiota composition, vitamin D_3 metabolisms and intestinal cytokine expression in food allergy (FA) mice. (a) FA mice received FMT with control donor feces (control-FMT, n=10). The phyla *Bacteroidetes* and *Firmicutes* were evaluated by quantitative real-time PCR. **, $P< 0.01$ *vs.* FA mice without FMT (n=5, Student's *t*-test). (b) Serum levels of vitamin D_3 or intestinal levels of sterol 27-hydroxylase (CYP27A1) and 25-hydroxyvitamin D_3-1α hydroxylase (CYP27B1) were evaluated by ELISA and quantitative real-time PCR, respectively. *, **, $P< 0.05$ and 0.01 *vs.* baseline or the indicated pair, respectively (Student's *t*-test). (c) Intestinal levels of IL-25, IL-33, thymic stromal lymphopoietin (TSLP) and nuclear factor erythroid 2-related factor 2 (Nrf2) were evaluated by quantitative real-time PCR. White bar: FA mice with Control-FMT, black bar: FA mice without FMT. *, **, $P< 0.05$ and 0.01 *vs.* baseline or the indicated pair, respectively (Student's *t*-test).

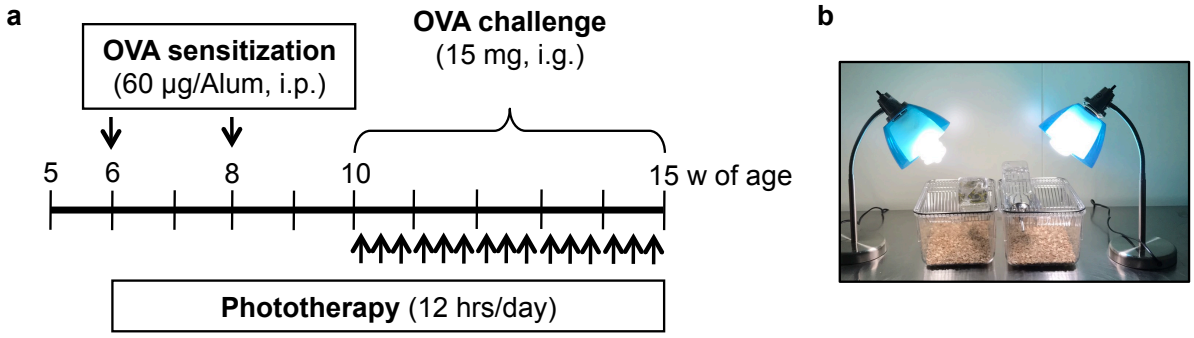

Supplementary Figure 9. Establishment of a food allergy (FA) model and phototherapy. (a) Schedule for establishment of the FA model. BALB/c mice were intraperitoneally (i.p.) immunized twice with a precipitate (100 μl/mouse) of ovalbumin (OVA, 60 μg) and aluminum hydroxide (Alum, 1 mg) followed by repeated intragastric (i.g.) OVA (15 mg in a final volume of 150 μl of PBS) challenge 15 times. (b) Artificial sunlight setting for phototherapy. The phototherapy group received daily exposure to artificial sunlight (color temperature 5500 K, color rendition indexes >90) (12 hours/day) throughout the entire experiment (9 weeks).

Supplementary Table 1. Primer information.

Primer	Sequence
IL-25	Forward: 5'-ACAGGGACTTGAATCGGGTC-3'
	Reverse: 5'-TGGTAAAGTGGGACGGAGTTG-3'
IL-33	Forward: 5'-GGCTGCATGCCAACGACAAGG-3'
	Reverse: 5'-AAGGCCTGTTCCGGAGGCGA-3'
TSLP	Forward: 5'-CCAGGCTACCCTGAAACTGA-3'
	Reverse: 5'-TCTGGAGATTGCATGAAGGA-3'
VDR	Forward: 5'-TGACTTTGACCGGAATGTGCCT-3'
	Reverse: 5'-TTCATCATGCCAATGTCCACGCAG-3'
CYP27A1	Forward: 5'-CAACCTCCTTTGGGACTTAC-3'
	Reverse: 5'-TGATCCATGTGGTCTCTTATTG-3'
CYP27B1	Forward: 5'-CGCTAGTCTCCCTATGTCACTATGC-3'
	Reverse: 5'-AGCCGAAGGGAAGAGATGC-3'
Nrf2	Forward: 5'-CTGAACTCCTGGACGGGACTA-3'
	Reverse: 5'-CGGTGGGTCTCCGTAAATG-3'
HO-1	Forward: 5'-AGCACTATGTAAAGCGTCTC-3'
	Reverse: 5'-CGGTCTTAGCCTCTTCTGT-3'
SOD1	Forward: 5'-AACCAGTTGTGTTGTCAGGAC-3'
	Reverse: 5'-CCACCATGTTTCTTAGAGTGAGG-3'
SOD2	Forward: 5'-TGGACAAACCTGAGCCCTAAG-3'
	Reverse: 5'-CCCAAAGTCACGCTTGATAGC-3'
β-actin	Forward: 5'-GGCTGTATTCCCCTCCATCG-3'
	Reverse: 5'-CCAGTTGGTAACAATGCCATGT-3'

Supplementary Table 2. Primer information.

Primer	Sequence
Bacteroidetes	Forward: 5'-GAAGGTCCCCCACATTG-3'
	Reverse: 5'-CGCKACTTGGCTGGTTCAG-3'
Firmicutes	Forward: 5'-GGAGYATGTGGTTTAATTCGAAGCA-3'
	Reverse: 5'-AGCTGACGACAACCATGCAC-3'
Total bacteria	Forward: 5'-ACTCCTACGGGAGGCAG-3'
	Reverse: 5'-GTATTACCGCGGCTGCTG-3'

nature research

Corresponding author(s): Toshiaki Nakano

Last updated by author(s): Feb 9, 2021

Reporting Summary

Nature Research wishes to improve the reproducibility of the work that we publish. This form provides structure for consistency and transparency in reporting. For further information on Nature Research policies, see our Editorial Policies and the Editorial Policy Checklist.

Statistics

For all statistical analyses, confirm that the following items are present in the figure legend, table legend, main text, or Methods section.

n/a	Confirmed	
☐	☒	The exact sample size (*n*) for each experimental group/condition, given as a discrete number and unit of measurement
☐	☒	A statement on whether measurements were taken from distinct samples or whether the same sample was measured repeatedly
☐	☒	The statistical test(s) used AND whether they are one- or two-sided *Only common tests should be described solely by name; describe more complex techniques in the Methods section.*
☒	☐	A description of all covariates tested
☒	☐	A description of any assumptions or corrections, such as tests of normality and adjustment for multiple comparisons
☐	☒	A full description of the statistical parameters including central tendency (e.g. means) or other basic estimates (e.g. regression coefficient) AND variation (e.g. standard deviation) or associated estimates of uncertainty (e.g. confidence intervals)
☒	☐	For null hypothesis testing, the test statistic (e.g. *F*, *t*, *r*) with confidence intervals, effect sizes, degrees of freedom and *P* value noted *Give P values as exact values whenever suitable.*
☒	☐	For Bayesian analysis, information on the choice of priors and Markov chain Monte Carlo settings
☐	☒	For hierarchical and complex designs, identification of the appropriate level for tests and full reporting of outcomes
☐	☒	Estimates of effect sizes (e.g. Cohen's *d*, Pearson's *r*), indicating how they were calculated

Our web collection on statistics for biologists contains articles on many of the points above.

Software and code

Policy information about availability of computer code

Data collection	No software was used.
Data analysis	FLASH (V1.2.7, http://ccb.jhu.edu/software/FLASH/) QIIME (V1.7.0, http://qiime.org/index.html) UCHIME algorithm (http://www.drive5.com/usearch/manual/uchime_algo.html)

For manuscripts utilizing custom algorithms or software that are central to the research but not yet described in published literature, software must be made available to editors and reviewers. We strongly encourage code deposition in a community repository (e.g. GitHub). See the Nature Research guidelines for submitting code & software for further information.

Data

Policy information about availability of data

All manuscripts must include a data availability statement. This statement should provide the following information, where applicable:

- Accession codes, unique identifiers, or web links for publicly available datasets
- A list of figures that have associated raw data
- A description of any restrictions on data availability

Raw data from the fecal microbiota analysis are deposited in the SRA database public repository from NCBI within the Bioproject accession number PRJNA690991.

Field-specific reporting

Please select the one below that is the best fit for your research. If you are not sure, read the appropriate sections before making your selection.

☒ Life sciences ☐ Behavioural & social sciences ☐ Ecological, evolutionary & environmental sciences

For a reference copy of the document with all sections, see nature.com/documents/nr-reporting-summary-flat.pdf

Life sciences study design

All studies must disclose on these points even when the disclosure is negative.

Sample size	Power analysis (G*Power, http://www.gpower.hhu.de) was performed for sample size calculation. We also check the reference (PLoS One 2012;7:e37156) to determine the sample size.
Data exclusions	No data were excluded from the data analyses.
Replication	We confirmed the reproducibility of the research findings.
Randomization	Animals were randomly divided into experimental groups.
Blinding	Group allocation/data collection and data analysis were performed by independent researchers.

Reporting for specific materials, systems and methods

We require information from authors about some types of materials, experimental systems and methods used in many studies. Here, indicate whether each material, system or method listed is relevant to your study. If you are not sure if a list item applies to your research, read the appropriate section before selecting a response.

Materials & experimental systems

n/a	Involved in the study
☐	☒ Antibodies
☒	☐ Eukaryotic cell lines
☒	☐ Palaeontology and archaeology
☐	☒ Animals and other organisms
☒	☐ Human research participants
☒	☐ Clinical data
☒	☐ Dual use research of concern

Methods

n/a	Involved in the study
☒	☐ ChIP-seq
☒	☐ Flow cytometry
☒	☐ MRI-based neuroimaging

Antibodies

Antibodies used	Mcpt-1 (Thermo Fisher Scientific, Cat No. 14-5503-82, clone RF6.1); IL-25 (Thermo Fisher Scientific, Cat No. MA1-41067, clone 68C1039.2); IL-33 (Thermo Fisher Scientific, Cat No. MA5-15773, clone 12H6D12); TSLP (Thermo Fisher Scientific, Cat No. PA5-20320); CYP27A1 (Thermo Fisher Scientific, Cat No. PA5-27946); CYP27B1 (Thermo Fisher Scientific, Cat No. PA5-79128); IgG1 (BD Biosciences, Cat No. 553440 and 553441, clone A85-1); IgG2a (BD Biosciences, Cat No. 553446 and 553388, clone R11-89 and R19-15); IgE (BD Biosciences, Cat No. 553413 and 553419, clone R35-72 and R35-118); Nrf2 (GeneTex, Cat No. GTX103322); β-Actin (Millipore, Cat No. MAB1501, clone C4)
Validation	Mcpt-1 (mouse, IHC); IL-25 (mouse, IHC); IL-33 (mouse, IHC); TSLP (mouse, IHC); CYP27A1 (mouse, IHC); CYP27B1 (mouse, IHC); IgG1 (mouse, ELISA); IgG2a (mouse, ELISA); IgE (mouse, ELISA); Nrf2 (mouse, WB); β-Actin (mouse, WB)

Animals and other organisms

Policy information about studies involving animals; ARRIVE guidelines recommended for reporting animal research

Laboratory animals	BALB/c mice, female, 4 weeks of age
Wild animals	The study did not involve wild animals.
Field-collected samples	The study did not involve samples collected from the field.
Ethics oversight	Kaohsiung Chang Gung Memorial Hospital

Note that full information on the approval of the study protocol must also be provided in the manuscript.